www.sciencemag.org/content/358/6360/215/suppl/DC1

Supplementary Materials for

Anti-Markovnikov alkene oxidation by metal-oxo–mediated enzyme catalysis

Stephan C. Hammer, Grzegorz Kubik, Ella Watkins, Shan Huang, Hannah Minges, Frances H. Arnold*

*Corresponding author. Email: frances@cheme.caltech.edu

Published 13 October 2017, *Science* **358**, 215 (2017)
DOI: 10.1126/science.aao1482

This PDF file includes:

This PDF file includes:

I. Materials and methods

(**A**) All chemicals and solvents were purchased from commercial suppliers (Sigma Aldrich, Alfa Aesar, Fisher Scientific) and used without additional purification. The following proteins were purchased: Lysozyme (Sigma-Aldrich, product number: L6876), DNase I (GOLDBIO, catalog number D-300-5) and alcohol dehydrogenase (recombinant, from *E. coli*, Sigma Aldrich, product number: 49641).

(**B**) ^{1}H, ^{13}C and ^{19}F NMR spectra were recorded on a Varian Inova 300 MHz or 500 MHz, or Bruker Prodigy 400 MHz instrument, in $CDCl_3$ and are referenced to the residual solvent peak. Data for ^{1}H NMR are reported in the conventional form: chemical shift (δ ppm), multiplicity (d = doublet, dd = doublet of doublets, t = triplet, q = quartet, m = multiplet), coupling constant (Hz), integration. Data for ^{13}C NMR are reported in terms of chemical shift (δ ppm), multiplicity (t = triplet, q = quartet).

(**C**) Analytical high-performance liquid chromatography (HPLC) was carried out on an Agilent 1260 Infinity instrument using a Poroshell 120 Eclipse column (Agilent, XDB C18, 4.6 x 5 mm, 2.7 μm) with H_2O and acetonitrile as the mobile phase. All measurements were performed with an Agilent 1260 Infinity Diode Array Detector and the wavelength at 210 nm was recorded. HPLC method for screening: Begin with 28% acetonitrile, hold for 0.3 min, linear gradient to 100% acetonitrile after 1.2 min, hold for 0.3 min, return to 28% acetonitrile from 1.5 to 1.6 min., hold for 0.75 min. Flowrate 2.5 mL/min. HPLC method for quantification: Begin with 10% acetonitrile, linear gradient to 75% acetonitrile after 7.5 min, linear gradient to 100% acetonitrile after 7.8 min, hold for 1.0 min, back to 10% acetonitrile from 8.8 to 8.9 min., keep for 1.4 min. Flowrate 1.5 mL/min. HPLC method for the quantification of α-methylstyrene and *trans*-β-methylstyrene conversions: Begin with 20% acetonitrile, linear gradient to 50% acetonitrile after 6.5 min, linear gradient to 75% acetonitrile after 7.5 min, linear gradient to 100% acetonitrile after 8.8 min, hold for 2.0 min, return to 20% acetonitrile from 10.8 to 10.9 min., hold for 1.4 min. Flowrate 1.5 mL/min.

(**D**) Gas chromatography (GC) analyses were conducted with a Shimadzu GC-17A instrument equipped with a flame ionization detector using an Agilent J&W HP-5 column (30 m x 0.32 mm, 0.25 μm film, part number 19091J-413) with helium as carrier gas. Injector temperature: 250°C. Split mode with a split ratio of 5. Detector temperature: 300°C. Oven temperature: 90 °C hold 2 min, 6 °C/min to 100 °C, 40 °C/min to 280°C hold 1 min, 9.17 min total.

(**E**) Chiral GC analysis was conducted with an Agilent 7820A instrument equipped with a flame ionization detector using an Agilent Cyclosil-B column (30 m x 0.32 mm, 0.25 μm film, part number 113-6632) with helium as carrier gas. Injector temperature: 200°C. Split mode with a split ratio of 5. Detector temperature: 300°C. Method for the separation of 2-phenylpropionaldehyde, oven temperature: Begin at 90 °C, 0.1 °C/min to 92.8 °C, 15 °C/min to 240 °C, hold 2 min. Method for the separation of 2-phenyl-1-propanol, oven temperature: Begin at 105 °C, 0.15 °C/min to 109.5 °C, 40 °C/min to 240 °C, hold 2 min. Method for the separation of 1-phenyl-2-propanol, oven temperature: Begin at 80 °C, hold 2 min, 8 °C/min to 120 °C, 12 °C/min to 170 °C, 15 °C/min to 240 °C, hold 5 min.

(**F**) $P450_{LA1}$ was cloned into a pET22b(+) vector containing a C-terminal 6xHis-tag. Gene and amino acid sequence of cytochrome $P450_{LA1}$ monooxygenase (Uniprot ID: A0P0F6) which was used as starting point for the directed evolution.

ATGGAACGCACTGCAAATCCAGCGGACGTTCCGGCTGGTGGTAAATCTTCTGAAGGCAAGGCGGGTACTCCACCGGCT
GCTGAAGCTCAATGCCCTTTCAGCAAAATGGCAGCAGATTTCGACGCTTTCGCAGGCCCATATCAGGCTGATCCGGCA
GAAGCGCTGCGTTGGTCTCGTGACCAGCTGCCGGTTTTCTATTCCCCGAACCTGGGTTACTGGGTGGTTTCTCGTTAC
GATGATATCAAAGCTGTTTTTCGTGACAACATCCTGTTCAGCCCGCGTAACGCTCTGGAAAAAATTACTCCGGCAACC
CCGGAAGCGATGGAGGTCCTGAAAGGTTATGGTTACGCAATGAACCGTACCATGGTTAACGAAGACGAACCAGTTCAC
ATGGAACGTCGTCGTGCACTGATGGGCCACTTCCTGCCGGACAATCTGGAAGCTCGTCAGGAGATGGTACGCCGCCTG
ACCCGCGAAAAAATCGATGCATTCATCGATTCCGGTCGCGTGGATCTGGTGGAAGCCATGCTGTATGAGGTTCCGCTG
AACGTTGCTCTGCACTTCCTGGGCGTTCCGGAGGATGACATTGCCATTCTGAAAAACTTTTCTGTCGCACACAGCGTC
AACACCTGGGGTAAACCGACCGATGAGCAGCAGGTTGCGATCGCACACGACGTTGGTCAGTTCTGGAACTATGCTGGT
AAAATCATCGAAAAAATGCGCAAGGAACCGGACGGTACCGGTTGGATGCACGAAACCATCCGTAAAAACGCAGAAATG
CCGGATATTGTTCCGGATTCTTATGTTCACTCCATGATGATGGCGATCATCGTTGCGGCACACGAGACCACCAGCCTG
GCCTCTGCAGGTATGTTTAAAACCCTGCTGACTCACCGTCAGGCTTGGCAGGATATCTGCGAGGACCCGTCCCTGATT
CCGAACGCAGTTGAGGAGTGTCTGCGTTATAGCGGCTCCATCGTGGCATGGCGTCGTCAAGCTACGGCTGCCACCCGT
ATCGGTGGTGTCGACATCCCGGAAGGTGCTAAACTGCTGATCGTTCAAGCATCTGGTAATCAGGATGAGCGTCACTTC
GAGGATGGTGACAAATTTGACATCTACCGCGATAACGCGGTGGACCACCTGACCTTTGGCTACGGTTCTCATCAGTGT
ATGGGCAAAAACATTGCCCGTATGGAGATGCGCATCTTTCTGGAAGAAATGACTCGTCGCCTGCCTCACCTGCAACTG
GCGGAACAGGAATTCACTTACCTGTCCAACACCAGCTTTCGTGGTCCGGATCATGTGTGGGTCGAATGGGATCCGGAA
AAAAACCCTGAACGTGCCGATCCGAGCCTGGCTAACGGCAACCACCGTTTTCCAGTTGGTGCCCCAGCCCGCCGTGAT
ATTGCACGTAAAATTCGCATCAAAACTGTTCGTCGTGAAGCCGACGGCATCCTGGGCCTGACCATTGAGGATGCAAAG
GGTCGTTCTCTGCCACGTTGGTCCGCTGGTGCGCACATCGAAGTGTGTGTTGACGGCTTCGACCGTAAATATTCCCTG
TGTGGTCGTGCGGACTCCCGTGACTATGATATCGCAGTTCTGCTGGAAGAAGGCGGTCGCGGTGGTAGCCGTCGTATT
CACGAAGTGGCTGCCGAGGGCCTGGAGCTGCGCCTGCGTGGTCCTTCTAACCTGTTCCGCCTGGACGAACAGGCGCGT
TCCTATGTTCTGATTGCGGGTGGCATTGGTATCACCCCGATCCTGGCAATGGCGGACCACCTGAAAGCCCTGGGTCGT
GACTACACCATCCACTACTGCGGTCGTTCTCGTCGTTCTATGGCATTCCTGGACCGTCTGCAGGCAGACCATGGCGAG
CGTCTGTCTGTGCATGCTGGCGATGAGAACCGTCACGCCGAGCTGGCTGGTATTGTTGCCTCCCTGCCGGAAGGTGGC
CAGATTTACGCATGTGGTCCGGAACGTATGATCAGCGAGCTGGAAGATCTGACCGCCCGTCTGCCACATGGCACCCTG
CATTTCGAGCACTTCAGCGCTCAGGAAACTGCCCTGGACCCGTCTAAAGAAAACGCATTCCAGGTAGAACTGAAAGAT
TCCGGTCTGACTCTGGAGGTGGCTGCGAACGTTACCCTGCTGGATGCACTGCTGGCGTCTGGTATCGATATCTCTTGT
GACTGCCGTGAAGGCCTGTGTGGCTCTTGCGAGGTAGAAGTCCTGGAGGGCGAGATCGACCACCGCGACGTGGTACTG
ACTCGCACCGAACGTGCGGAAAACCGTCGCATGATGTCTTGCTGTTCCCGCTCTGTAAAAGGCGGTAAGCTGAAACTG
GCACTGCTCGAGCACCACCACCACCACCACTGA

MERTANPADVPAGGKSSEGKAGTPPAAEAQCPFSKMAADFDAFAGPYQADPAEALRWSRDQLPVFYSPNLGYWVVSRY
DDIKAVFRDNILFSPRNALEKITPATPEAMEVLKGYGYAMNRTMVNEDEPVHMERRRALMGHFLPDNLEARQEMVRRL
TREKIDAFIDSGRVDLVEAMLYEVPLNVALHFLGVPEDDIAILKNFSVAHSVNTWGKPTDEQQVAIAHDVGQFWNYAG
KIIEKMRKEPDGTGWMHETIRKNAEMPDIVPDSYVHSMMMAIIVAAHETTSLASAGMFKTLLTHRQAWQDICEDPSLI
PNAVEECLRYSGSIVAWRRQATAATRIGGVDIPEGAKLLIVQASGNQDERHFEDGDKFDIYRDNAVDHLTFGYGSHQC
MGKNIARMEMRIFLEEMTRRLPHLQLAEQEFTYLSNTSFRGPDHVWVEWDPEKNPERADPSLANGNHRFPVGAPARRD
IARKIRIKTVRREADGILGLTIEDAKGRSLPRWSAGAHIEVCVDGFDRKYSLCGRADSRDYDIAVLLEEGGRGGSRRI
HEVAAEGLELRLRGPSNLFRLDEQARSYVLIAGGIGITPILAMADHLKALGRDYTIHYCGRSRRSMAFLDRLQADHGE
RLSVHAGDENRHAELAGIVASLPEGGQIYACGPERMISELEDLTARLPHGTLHFEHFSAQETALDPSKENAFQVELKD
SGLTLEVAANVTLLDALLASGIDISCDCREGLCGSCEVEVLEGEIDHRDVVLTRTERAENRRMMSCCSRSVKGGKLKL
ALLEHHHHHH

(**G**) Gene and amino acid sequence of the *anti*-Markovnikov oxygenase (aMOx).

ATGGAGCGCACTGCAAATCCAGCGGACGTTCCGGCTGGTGGTAAATCTTCTGAAGGCAAGGCGGGTACTCCACCGGCT
GCTGAAGCTCAATGCCCTTTCAGCAAAATGGCAGCAGATTTCGACGCTTTCGCAGGCCCATATCAGGCTGATCCGGCA
GAAGCGCTGCGTTGGTCTCGTGACCAGCTGCCGGTTTTCTATTCCCCGAACCTGGGTTACTGGGTGGTTTCTCGTTAC
GATGATATCAAAGCTGTTTTTCGTGACAACATCCTGTTCAGCCCGCGTAACGCTCTGGAAAAAATCACTCCGCTGACC
CCGGAAGCGATGGAGGTCCTGAAAGGTTATGGTTACGCACTGAACCATGCCATGATTAACGAAGACGAACCAGTTCAC
ATGGAACGTCGTCGTGCACTGATGGGCCACTTCCTGCCGGACAATCTGGAAGCTCGTCAGGAGATGGTACGCCGCCTG
ACCCGCGAAAAAATCGATGCATTCATCGATTCCGGTCGCGTGGATCTGGTGGAAGCCATGCTGTATGAGGTTCCACTG
AACGTTGCCCTGCACTTCCTGGGCGTTCCGGAGGATGACATTGCCATTCTGAAAAAGTTTTCTGTCGCACACAGCGTC
AGCACCTGGGGTAAACCGACCGATGAGCAGCAGGTTGCGATCGCACACGACGTTGGTCAGTTCTGGAACTATGCTGGT
AAAATCATCGAAAAAATGCGCAAGGAACCGGACGGTACCGGTTGGATGCACGAAACCATCCGTAAAAACGCAGAAATG
CCGGATATTGTCCCGGATTCTTATGTTCACTCCATGATGATGGCGATCATCGTTGCGGCACACGAGACCACCAGCCTG
GCCTCTGCAGGTATGTTTAAAACCCTGCTGACTCACCGTCAGGCTTGGCAGGATATCTGCGAGGACCCGTCTCTGATT
CCGAACGCAGTTGAGGAGTGTCTGCGTTATAGCGGCTCCGTTATGGCATGGCGTCGTCAAGCTACGGCTGCCACCCGT
ATCGGTGGTGTCGACATCCCGGAAGGTGCTAAACTGCTGATCGTTCAAGCATCTGGTAATCAGGATGAGCGTCACTTC
GAGGATGGTGACAAATTTGACATCTACCGCGATAACGCGGTGGACCACCTGACCTTTGGCGTGGGTTCTCACCAGTGT
CTGGGCAAAAACATTGCCCGTATGGAGATGCGCATCTTTCTGGAAGAAATGACTCGTCGCCTGCCTCACCTGCAACTG
GCGGGACAGGAATTCACTTACCTGTCCAACACCAGCTTTCGTGGTCCGGATCATGTGTGGGTCGAATGGGATCCGGAA
AAAAACCCTGAACGTGCCGATCCGAGCCTGGCTAACGGCAACCACCGTTTTCCAGTTGGTGCCCCAGCCCGCCGTGAT
ATTGCACGTAAAATTCGCATCAAAACTGTTCGTCGTGAAGCCGACGGCATCCTGGGCCTGACCATTGAGGATGCAAAG
GGTCGTTCTCTGCCACGTTGGTCCGCTGGTGCGCACATCGAAGTGTGTGTTGACGGCTTCGACCGTAAATATTCCCTG
TGTGGTCGTGCGGACTCCCGTGACTATGATATCGCAGTTCTGCTGGAAGAAGGCGGTCGCGGTGGTAGCCGTCGTATT
CACGAAGTGGCTGCCGAGGGCCTGGAGCTGCGCCTGCGTGGTCCTTCTAACCTGTTCCGCCTGGACGAACAGGCGCGT
TCCTATGTTCTGATTGCGGGTGGCATTGGTATCACCCCGATCCTGGCAATGGCGGACCACCTGAAAGCCCTGGGTCGT
GACTACACCATCCACTACTGCGGTCGTTCTCGTCGTTCTATGGCATTCCTGGACCGTCTGCAGGCAGACCATGGCGAG
CGTCTGTCTGTGCATGCTGGCGATGAGAACCGTCACGCCGAGCTGGCTGGTATTGTTGCCTCCCTGCCGGAAGGTGGC
CAGATTTACGCATGTGGTCCGGAACGTATGATCAGCGAGCTGGAAGATCTGACCGCCCGTCTGCCACATGGCACCCTG
CATTTCGAGCACTTCAGCGCTCAGGAAACTGCCCTGGACCCGTCTAAAGAAAACGCATTCCAGGTAGAACTGAAAGAT
TCCGGTCTGACTCTGGAGGTGGCTGCGAACGTTACCCTGCTGGATGCACTGCTGGCGTCTGGTATCGATATCTCTTGT
GACTGCCGTGAAGGCCTGTGTGGCTCTTGCGAGGTAGAAGTCCTGGAGGGCGAGATCGACCACCGCGACGTGGTACTG
ACTCGCACCGAACGTGCGGAAAACCGTCGCATGATGTCTTGCTGTTCCCGCTCTGTAAAAGGCGGTAAGCTGAAACTG
GCACTGCTCGAGCACCACCACCACCACCACTGA

MERTANPADVPAGGKSSEGKAGTPPAAEAQCPFSKMAADFDAFAGPYQADPAEALRWSRDQLPVFYSPNLGYWVVSRY
DDIKAVFRDNILFSPRNALEKITPLTPEAMEVLKGYGYALNHAMINEDEPVHMERRRALMGHFLPDNLEARQEMVRRL
TREKIDAFIDSGRVDLVEAMLYEVPLNVALHFLGVPEDDIAILKKFSVAHSVSTWGKPTDEQQVAIAHDVGQFWNYAG
KIIEKMRKEPDGTGWMHETIRKNAEMPDIVPDSYVHSMMMAIIVAAHETTSLASAGMFKTLLTHRQAWQDICEDPSLI
PNAVEECLRYSGSVMAWRRQATAATRIGGVDIPEGAKLLIVQASGNQDERHFEDGDKFDIYRDNAVDHLTFGVGSHQC
LGKNIARMEMRIFLEEMTRRLPHLQLAGQEFTYLSNTSFRGPDHVWVEWDPEKNPERADPSLANGNHRFPVGAPARRD
IARKIRIKTVRREADGILGLTIEDAKGRSLPRWSAGAHIEVCVDGFDRKYSLCGRADSRDYDIAVLLEEGGRGGSRRI
HEVAAEGLELRLRGPSNLFRLDEQARSYVLIAGGIGITPILAMADHLKALGRDYTIHYCGRSRRSMAFLDRLQADHGE
RLSVHAGDENRHAELAGIVASLPEGGQIYACGPERMISELEDLTARLPHGTLHFEHFSAQETALDPSKENAFQVELKD
SGLTLEVAANVTLLDALLASGIDISCDCREGLCGSCEVEVLEGEIDHRDVVLTRTERAENRRMMSCCSRSVKGGKLKL
ALLEHHHHHH

II. General procedures

(**A**) **Cloning and library creation**. pET22b(+) was used as a cloning and expression vector for all enzymes and variants described in this study. The *E. coli* codon optimized $P450_{LA1}$ gene (Uniprot ID: A0P0F6) was ordered from IDT containing a C-terminal 6xHis-tag. Random mutagenesis of P450's heme domain was performed by error-prone PCR using varying $MnCl_2$ concentrations. The resulting PCR products were digested with *Dpn*I, purified by agarose gel electrophoresis and ligated into the pET22b(+) vector backbone by Gibson assembly (*45*). After an additional DNA purification step the plasmids were transformed *via* electroporation into *E. cloni* strain BL21(DE3). Site-saturation libraries were generated employing the "22c-trick" method (*46*). The PCR products were gel purified, digested with *DpnI*, ligated using the Gibson assembly Mix, and used to directly transform *E. cloni* strain BL21(DE3).

(**B**) **Expression of P450 libraries in 96-well plates**. The expression and screening of P450 variants was performed in 96-well plate format. Individual colonies from P450 libraries were cultivated in 500 µL of Terrific Broth medium (100 µg mL^{-1} ampicillin final concentration) for 20 h at 37 °C, 250 rpm using humidity control. Expression cultures were inoculated with 50 µL of preculture into 610 µL of Terrific Broth medium (100 µg mL^{-1} ampicillin final concentration). The cultures were incubated for 4 h at 37 ºC, 250 rpm, then cooled on ice for 10 min before induction (0.2 mM IPTG, 0.5 mM aminolevulinic acid, final concentration). Induced cells were shaken for 20 h at 25 ºC, 250 rpm. The cells were harvested (4500×g, 5 min, 4 ºC) and stored at -20 °C for three days.

(**C**) **Screening of random mutagenesis libraries using the Purpald assay**.(*47*) Buffer (0.1 M NaH_2PO_4, pH 8.0, 0.15 M NaCl, 0.5% glycerol by weight, 1.0 mg/mL lysozyme, 0.2 mg/mL DNase, 300 µL/well) was added to the cell pellet and lysis was performed by incubating 4 h at 4 °C, 150 rpm. The plate was centrifuged (4000×g, 4 °C, 10 min) and 100 µL of lysate were transferred with an automated liquid handling workstation to 96-well assay plates containing 5 µL styrene/DMSO stock solution and 100 µL NADH stock solution in buffer (10 mM styrene, 3.3 mM NADH final concentration). The plates were incubated for 2 h at 20 °C, 200 rpm. Purpald dissolved in 2 M NaOH (31 mM, 50 µL/well) was added and the plate was incubated for 30 min at room temperature. Aldehyde activity was analyzed by measuring the absorbance at 538 nm. 1500-2500 variants were screened per generation.

(**D**) **HPLC screening of site-saturation libraries**. Buffer (0.1 M NaH_2PO_4, pH 8.0, 0.15 M NaCl, 2% glycerol by weight, 1.0 mg/mL lysozyme, 0.2 mg/mL DNase, 300 µL/well) was added to the cell pellet and lysis was performed by incubating 4 h at 4 °C,150 rpm. The plate was centrifuged (4000×g, 4 °C, 10 min) and 150 µL of lysate were transferred with an automated liquid handling workstation to 96-well plate containing 10 µL styrene stock solution (15 mM final concentration in DMSO) and 250 µL NADPH/ADH stock solution (2 mM NADPH final concentration, 1 U/mL final conc. for ADH from Sigma Aldrich No. 49461). The plate was incubated for 1.5 h at 23 °C, 200 rpm. The reactions were diluted with 600 µL acetonitrile and incubated for 30 min at room temperature. The plate was centrifuged (4000 g, 4 °C, 5 min) and 150 µL of the supernatant were transferred to a 96-well assay plate. The amount of phenylethanol and styrene oxide was analyzed using analytical HPLC. 90 variants per site-saturation library were screened.

(**E**) **Large scale expression of P450 variants**. *E. coli* BL21(DE3) cells transformed with plasmid encoding P450 variants were grown overnight in 5 mL Luria-Bertani medium (100 ug mL^{-}

[1] ampicillin final concentration) at 37 ºC, 250 rpm. Expression cultures were inoculated with 5 mL of preculture into 500 mL Terrific Broth medium (100 μg mL^{-1} ampicillin final concentration) in a 2 L flask and incubated for 4 h at 37 ºC, 125 rpm. The flask was cooled on ice for 10 min before expression was induced (0.2 mM IPTG, 0.5 mM aminolevulinic acid, final concentration). Induced cells were shaken for 20 h at 25 ºC, 125 rpm. The cells were harvested (4500×g, 5 min, 4 ºC) and stored at -20 °C.

(**F**) **Bioconversions and determination of total turnover numbers**. Styrene was converted in an enzyme cascade together employing the P450 variant and alcohol dehydrogenase to determine the performance of each variant (total turnover number and *anti*-Markovnikov selectivity). Because aldehydes are prone to side reaction in buffered systems, we chose to combine our P450 with an alcohol dehydrogenase to prevent aldehyde accumulation by direct reduction to the corresponding alcohol. *E. coli* BL21(DE3) cells were lysed with lysis buffer (0.1 M NaH_2PO_4, pH 8.0, 0.15 M NaCl, 2% glycerol by weight, 1.0 mg/mL lysozyme, 0.2 mg/mL DNase) for 4 h on ice followed by centrifugation (30 min, 4000×g, 4 °C). The supernatant was used as lysate in the bioconversion reactions of styrene and other substrates. The concentration of P450 enzymes in lysate was determined from ferrous carbon monoxide binding difference spectra using the previously reported protocol (*48*). For bioconversions, 50 μL of lysate (approx. 0.3 μM P450 final conc.) were mixed with 742 μL $NADP^+$ buffer solution (0.1 M NaH_2PO_4, pH 8.0, 0.15 M NaCl, 2% glycerol by weight, 1 mM $NADP^+$ final conc.) containing 10 U ADH (Sigma Aldrich No. 49461) and 1 % isopropanol for NADPH cofactor regeneration. 8 μL substrate stock in DMSO (5 mM final substrate conc.) were added to start the reaction in 2 mL screw-top glass vials. The bioconversion was stopped by adding 800 μL acetonitrile after incubating 2 h at room temperature (400 rpm). The sample was incubated for 30 min at room temperature, centrifuged for 5 min. (14000×g, 25 °C) and the supernatant was analyzed by analytical HPLC. Calibration curves were determined for quantitative HPLC analysis using commercially available, authentic standards. The total turnover numbers (TTN) were calculated as ratio of product and P450 concentrations. The *anti*-Markovnikov selectivity was calculated by conc. alcohol / (conc. alcohol + conc. epoxide). The reactions were performed in triplicate from at least two biological replicates. For chiral GC measurements, the reaction was stopped after 2 h by extracting two times with 500 μL ethyl acetate, combined and used for analysis.

(**G**) **$P450_{LA1}$ purification**. *E. coli* BL21(DE3) cells were lysed with lysis buffer (3 mL / g cell pellet, 0.1 M NaH_2PO_4, pH 8.0, 0.15 M NaCl, 10% glycerol by weight, 10 mM imidazole, 1.0 mg/mL lysozyme, 0.2 mg/mL DNase) for 4 h on ice followed by centrifugation (35 min, 20,000×g, 4 °C). The protein containing a C-terminal 6xHis-tag was purified by loading the supernatant on a nickel NTA column (1 mL HisTrap HP, GE Healthcare, Piscataway, NJ) using an AKTA purifier. The column was washed with 4 column volumes buffer A (0.1 M NaH_2PO_4, pH 8.0, 0.15 M NaCl, 10% glycerol by weight, 10 mM imidazole) and the protein was eluted using a linear gradient from 100% buffer A to 100% buffer B (0.1 M NaH_2PO_4, pH 8.0, 0.15 M NaCl, 10% glycerol by weight, 10 mM imidazole) over 10 column volumes. The combined fractions were dialyzed with 3 L buffer (0.1 M NaH_2PO_4, pH 8.0, 0.15 M NaCl, 10% glycerol by weight) and concentrated. 50 μL aliquots were frozen using liquid nitrogen and stored and -20°C.

III. Supporting Figs. S1 to S11

Fig. S1 Summary of catalytic strategies for direct and sequential *anti*-Markovnikov oxidation of alkenes.

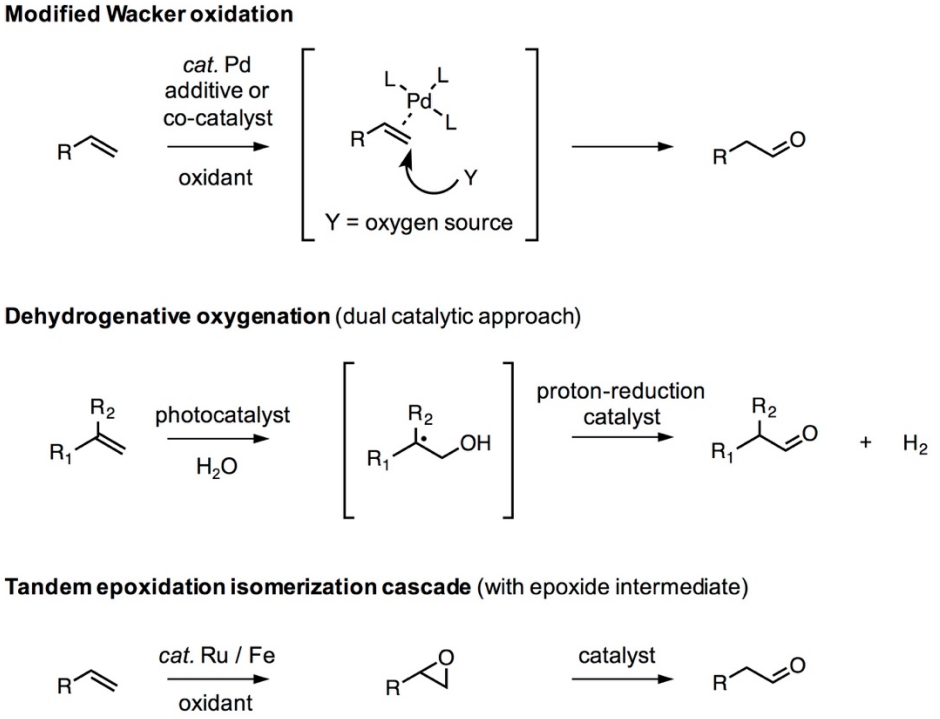

Catalytic protocols for *anti*-Markovnikov oxidation follow three major strategies: a modified Wacker oxidation, a dehydrogenative oxygenation approach, and a tandem epoxidation isomerization cascade. Strictly speaking, the tandem epoxidation-isomerization cascade is not a direct *anti*-Markovnikov oxidation. This cascade proceeds in a sequential manner via an epoxide intermediate that is rearranged in a second step. All current protocols either depend on precious metals performing with low turnover numbers (*29*, *49–60*) often combined with substrates bearing directing groups (*58–60*), do not offer enantiocontrol (*29*, *49–63*), utilize complex catalysts that require multistep synthesis (*56*, *61*) and/or use stoichiometric amounts of terminal oxidants such as iodosylbenzene which generate stoichiometric amounts of waste (*29*, *49*, *55*, *57*, *59–62*). Catalysts that use earth-abundant metals for aerobic direct *anti*-Markovnikov oxidation are unknown, and enantioselective *anti*-Markovnikov oxidations are out of reach (**Table S1**).

Fig. S2 Selectivity in the metal-oxo-mediated *anti*-Markovnikov oxidation of alkenes.

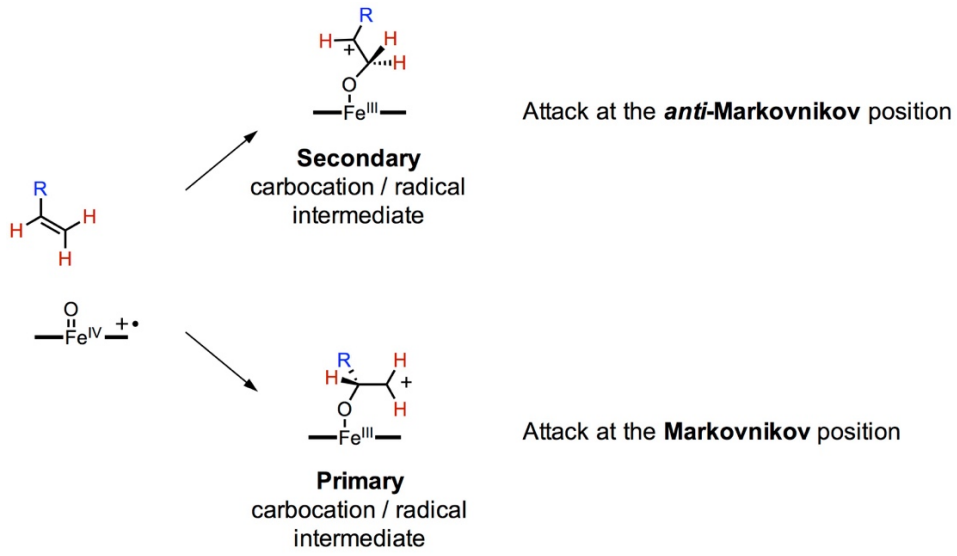

The *anti*-Markovnikov selectivity in this reaction is most likely a consequence of the relative energies of the high-energy intermediates in the catalytic cycle. The *anti*-Markovnikov reaction proceeds via the more stabilized secondary carbocation / radical intermediates. Markovnikov selectivity could be achieved via the less-stabilized primary carbocation / radical intermediates. However, Markovnikov oxidation products have not been observed.

Fig. S3 The **P450$_{LA1}$**-catalyzed *anti*-Markovnikov oxidation is a direct oxidation without an epoxide intermediate.

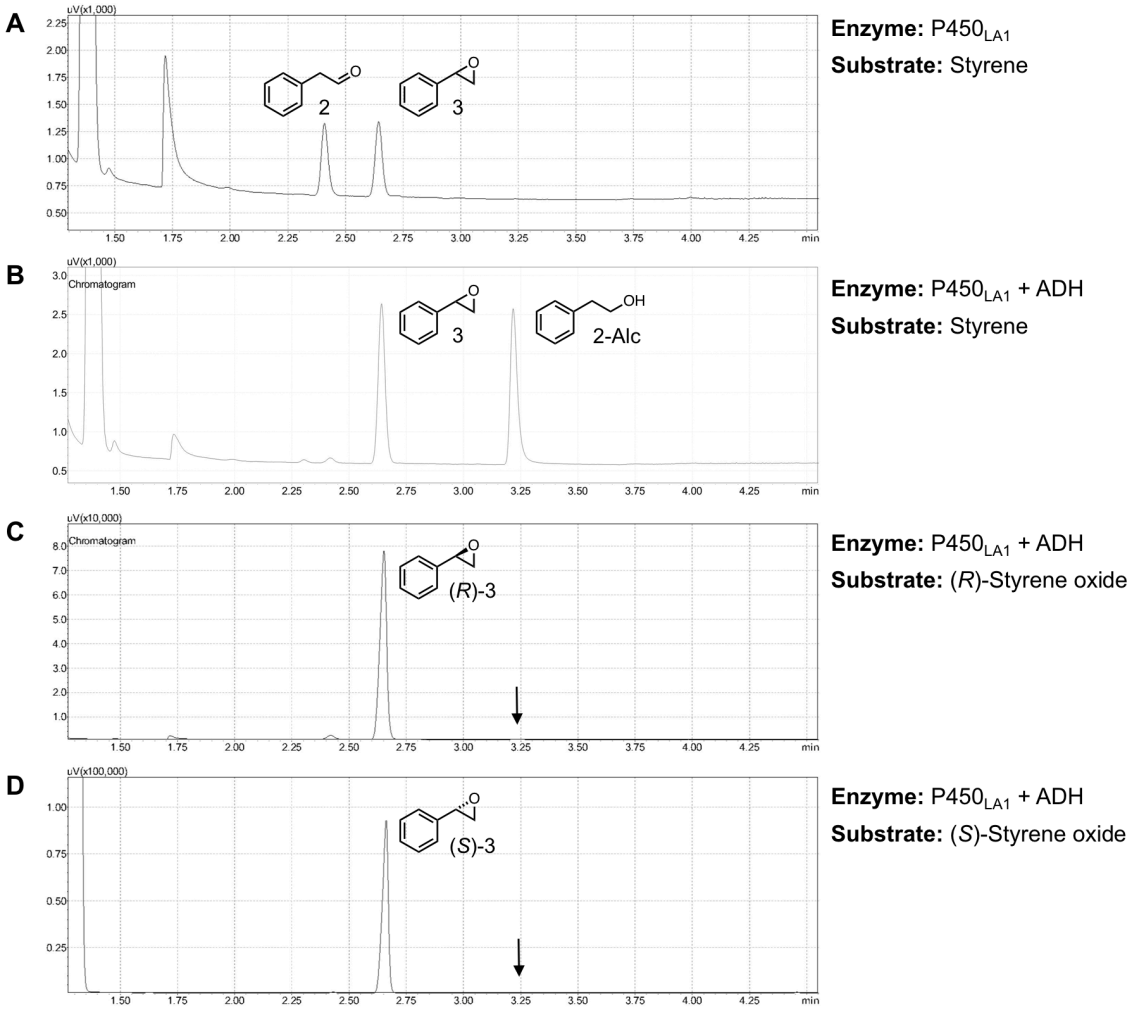

(**A**) GC chromatogram after conversion of styrene with P450$_{LA1}$. The reaction yields the corresponding phenylacetaldehyde **2** and styrene oxide **3**. (**B**) Same reaction as A, but in the presence of an alcohol dehydrogenase (ADH). The ADH reduces phenylacetaldehyde **2** to the corresponding 2-phenylethanol **2-Alc** and recycles the cofactor by isopropanol oxidation. Chromatograms in (**C**) and (**D**) are derived from the conversion of (*R*)- and (*S*)-styrene oxide. Neither epoxide enantiomer was converted using the P450$_{LA1}$ ADH cascade, thus demonstrating that epoxides are not substrates for P450$_{LA1}$ and not intermediates in the catalytic cycle. Thus, P450$_{LA1}$ catalyzes a direct *anti*-Markovnikov oxidation and not an epoxidation-isomerization sequence as suggested previously (*18*).

Fig. S4 Purpald assay for high-throughput colorimetric aldehyde quantification.

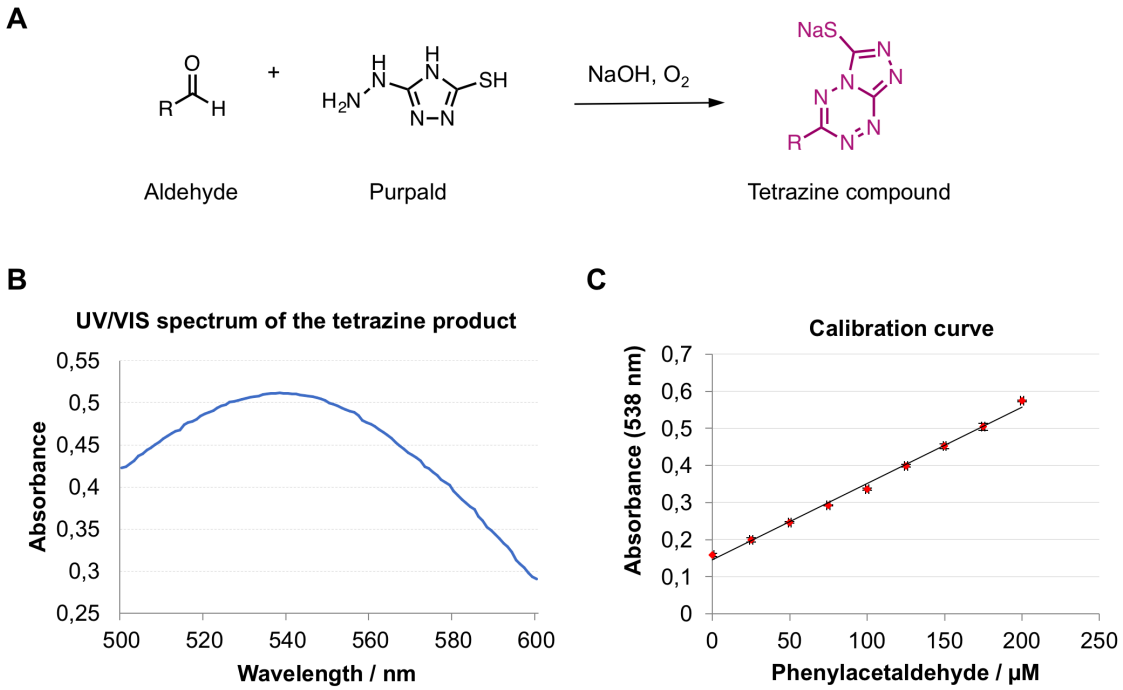

(**A**) The Purpald reagent (*47*) was used to quantify aldehyde concentration in high-throughput. Purpald forms a cyclic aminal with aldehydes that rapidly get oxidized to the corresponding purple-colored tetrazine. (**B**) The UV/VIS spectrum of the tetrazine product shows a maximum at 538 nm, which was used as the absorbance wavelength in the assay. (**C**) Tetrazine formation, measured as absorbance (538 nm), shows linear dependence on the phenylacetaldehyde concentration.

Fig. S5 Predicted protein structure of the $P450_{LA1}$ heme domain.

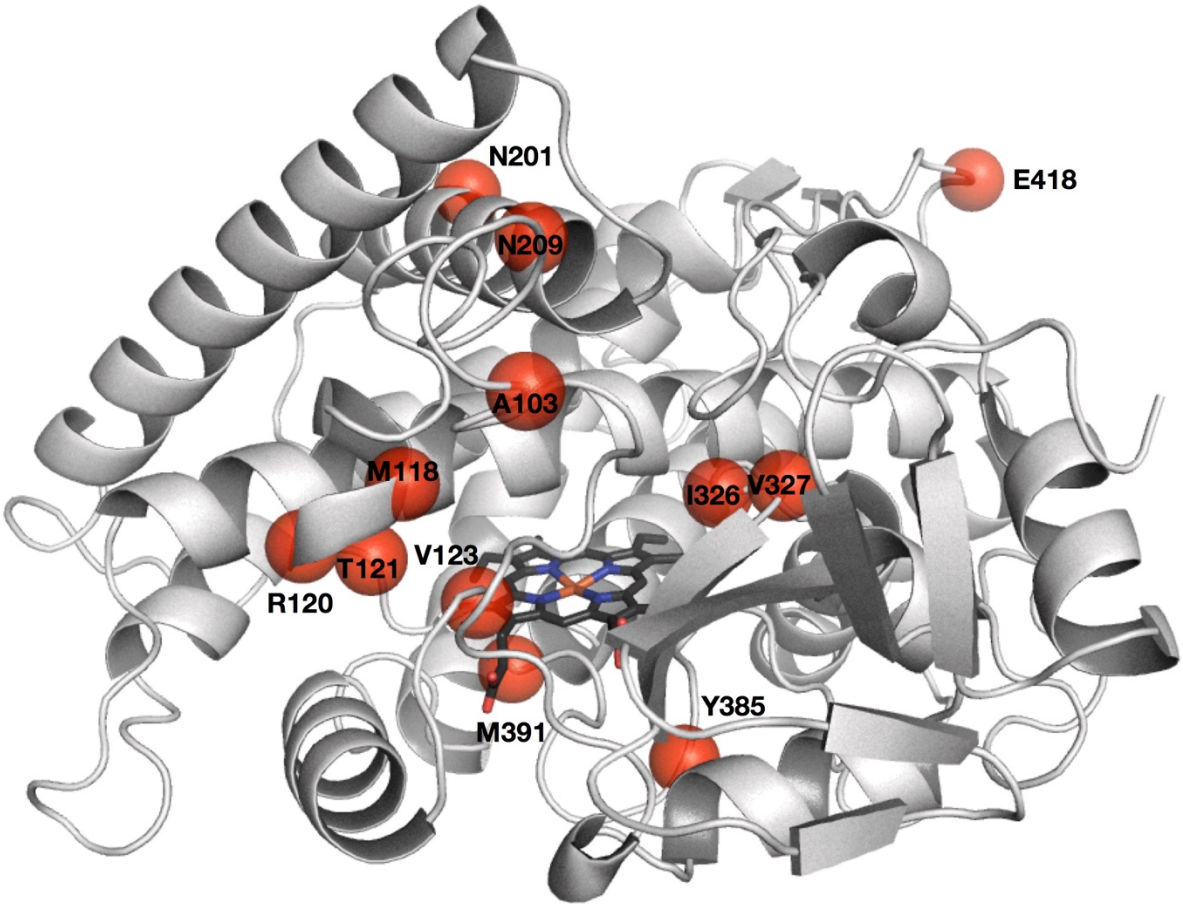

The structure of the $P450_{LA1}$ heme domain was predicted using I-Tasser (*64*), SWISS-MODEL (*65*) and Phyre2 (*66*). The $P450_{LA1}$ heme domain has low sequence identity (<50%) with structurally characterized P450s. The structure prediction tools generated models based on the structures of the P450 monooxygenase PikC (PDB ID: 2WHW) (*67*) and a P450 from *Streptomyces peucetius* (PDB ID: 5IT1) (*68*). The mutations identified in the screening of random mutagenesis libraries are distributed over the heme domain (T121A, N201K, N209S, Y385H and E418G). All five mutations contribute to the improved activity, but only the T121A mutation, believed to be in the active site based on these homology models, significantly enhanced selectivity for the *anti*-Markovnikov product (from 45% to 55%). These homology models were used to identify potential active site amino acids for iterative site-saturation mutagenesis (*21*). The following potential active site amino acids were mutated and screened during the course of laboratory evolution: L97, A103, Y116, A117, M118, N119, R120, A121, M122, V123I, N124, H206, S207, A275, V278, S325, I326, V327, W329, R330, S428 and F429 (see Table S2 for more details). In addition, the highly conserved amino acids of the heme binding site (Cys ligand loop) were targeted for site-saturation mutagenesis: F383, G384, Y385 (H385 in $P450_{LA1}$ wild type), G386, S387, H388, Q389, M391, G392 and K393.

Fig. S6 The **aMOx**-catalyzed *anti*-Markovnikov oxidation is a direct oxidation without an epoxide intermediate.

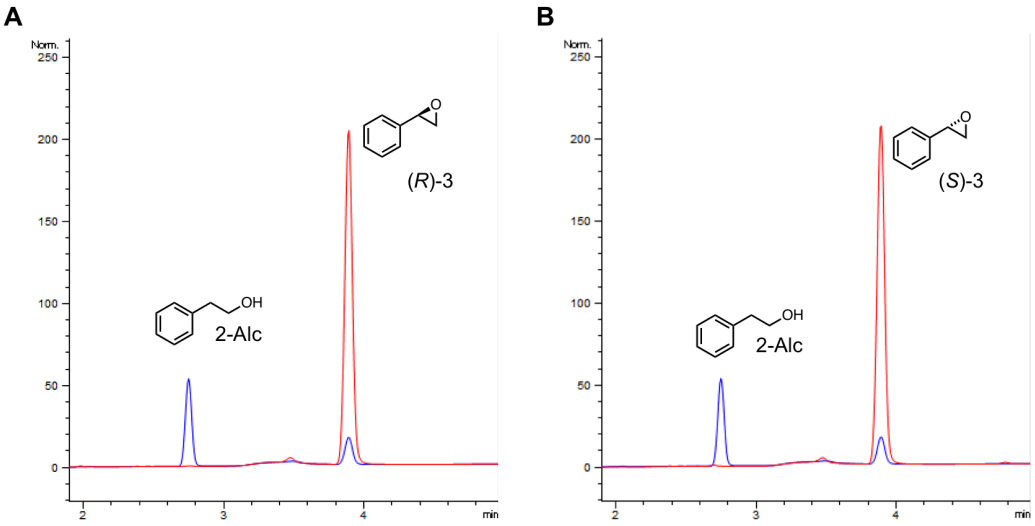

$P450_{LA1}$ wild type did not show any epoxide aldehyde isomerization activity (see Fig. S3). To prove that laboratory evolution did not generate isomerization activity, the corresponding (*R*)- and (*S*)-epoxides were incubated with aMOx using the standard biotransformation protocol. This standard protocol includes an alcohol dehydrogenase and cofactor recycling system to reduce the generated aldehyde to the corresponding alcohol **2-alc**. Since neither the (*R*)- nor the (*S*)-epoxide enantiomer were converted under these conditions, the epoxide is not an intermediate of the catalytic cycle. (**A**) HPLC chromatogram of a sample (blue) containing phenylethanol **2-Alc** and styrene oxide **3** is compared to the biotransformation of (*R*)-3 (red). No aldehyde or alcohol formation was observed. (**B**) HPLC chromatogram of a sample (blue) containing phenylethanol **2-Alc** and styrene oxide **3** is compared to the biotransformation of (*S*)-3 (red). No aldehyde or alcohol formation was observed.

Fig. S7 Time course for conversion of styrene to products.

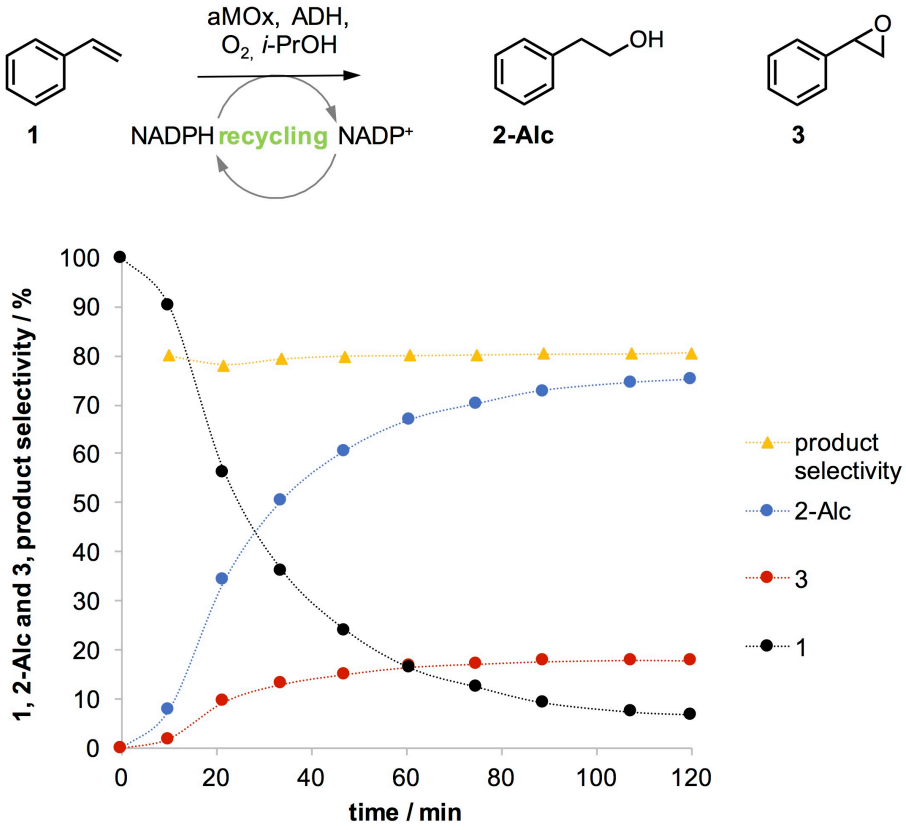

Conversion of styrene **1** with aMOx. Since aldehydes are prone to side reactions in water, the aldehyde product of the aMOx reaction was directly converted to the corresponding alcohol **2-alc** using an enzyme cascade with an alcohol dehydrogenase (ADH). The ADH has dual function in that it also recycles the NADPH cofactor by isopropanol oxidation. The time course of the reaction demonstrates constant product selectivity for **2-Alc** and **3** (yellow triangles), which supports the proposed mechanism of direct *anti*-Markovnikov oxidation without an epoxide intermediate. Reaction conditions: 2 mM alkene, 1.0 µM aMOx, 10 units ADH, 1% *i*-PrOH, 0.2 equiv. $NADP^+$, 2 h reaction time at room temperature.

Fig. S8 Isotopic labeling experiment.

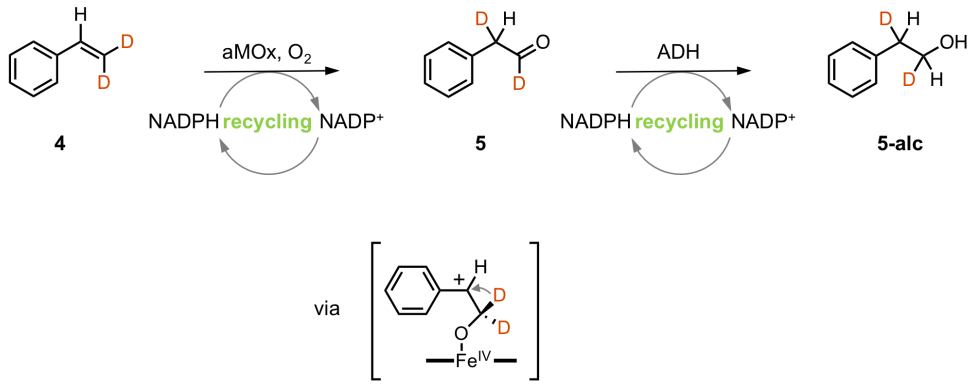

To confirm that a 1,2-hydride shift is part of the aMOx cycle, deuterium-labeled styrene **4** was used as substrate. Since aldehydes are prone to racemization in buffered medium, the aldehyde product **5** of the aMOx step was directly converted to the corresponding alcohol **5-alc** using an enzyme cascade with an alcohol dehydrogenase. The deuterated styrene **4** showed conversion and *anti*-Markovnikov selectivity identical to the non-deuterated styrene. The isolated alcohol product **5-alc** was analyzed by NMR and compared to a commercial standard without deuterium label. The ^{1}H NMR spectrum of the isotopically labeled alcohol product clearly shows an integral of only one H at the benzylic position (see NMR spectra below). In addition, the ^{13}C NMR spectra reveal a triplet for the benzylic carbon which is in accordance with C-D coupling.

For the biotransformation, 4.2 mL *E. coli* lysate (for preparation see general procedures, 0.25 µM final aMOx conc.) were mixed with 81.2 mL $NADP^+$ buffer solution (0.1 M NaH_2PO_4, pH 8.0, 0.15 M NaCl, 2% glycerol by weight, 500 µM $NADP^+$ final conc.), containing 600 U ADH (Sigma Aldrich No. 49461) and 1 % isopropanol for NADPH cofactor regeneration. 0.85 µL styrene-β,β-d_2 substrate stock in DMSO (5 mM final substrate conc.) were added to start the reaction. The bioconversion was incubated 1 h at 23°C (200 rpm). The crude product was extracted with 75 mL of a 1:1 mixture ethyl acetate / *n*-hexane (three times). The combined organic phase was dried with $MgSO_4$ and the solvent was removed under reduced pressure. The isolated oil was purified by with column chromatography using silica gel (ethyl acetate : *n*-hexane = 1:10 to 1:4, v:v) to yield 5-alc (7.5 mg, 14%) as colorless oil. ^{1}H NMR (300 MHz, $CDCl_3$) δ 7.45-7.27 (m, 2H), 7.29-7.06 (m, 3H), 3.88-3.81 (m, 1H), 2.90-2.82 (t, J = 6.4 Hz, 1H). ^{13}C NMR (100 MHz, $CDCl_3$) δ 138.39, 129.02 (2C), 128.60 (2C), 126.49, 63.29 (t), 38.74 (t) ppm.

Fig. S9 aMOx-catalyzed enantioselective *anti*-Markovnikov oxidation of α-methylstyrene.

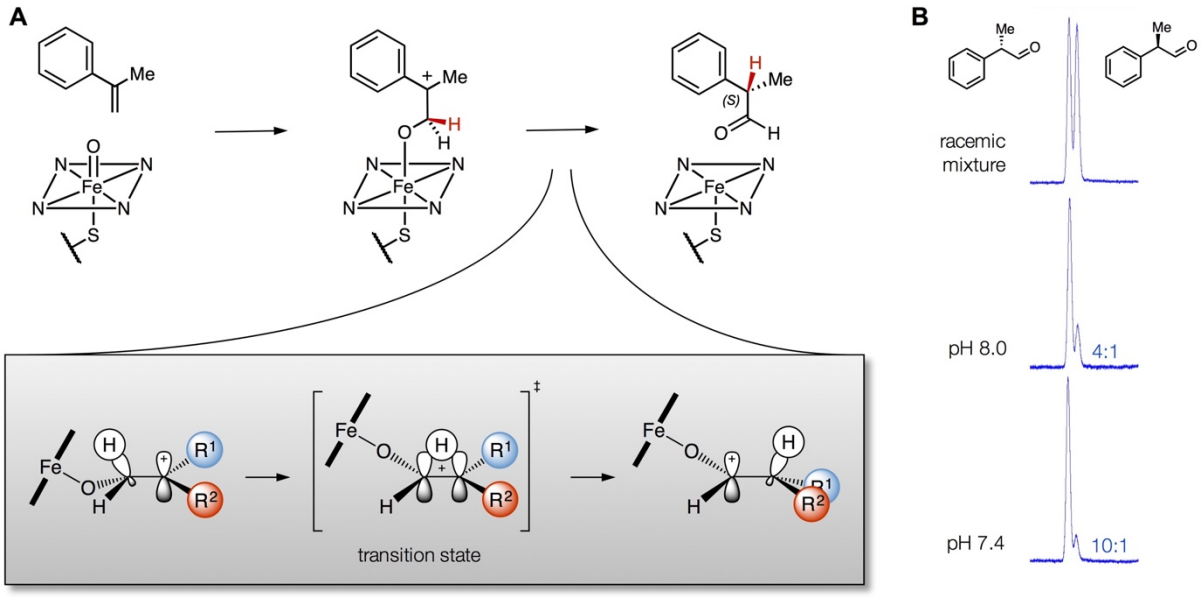

(**A**) Proposed mechanism for the *anti*-Markovnikov oxidation of alkenes. Since isotopic labeling confirmed a 1,2-hydride migration as part of the catalytic cycle, we propose that the stereocenter is generated by controlling the enantioselectivity of the 1,2-migration. The enzyme can achieve this by locking the substrate in a specific conformation that pre-aligns the orbitals for the carbocation 1,2-rearrangement. This suprafacial 1,2-shift (grey box) is believed to proceed in a concerted fashion (*25*, *44*). (**B**) Traces of chiral gas chromatography analyses are compared. Racemic mixture (top), enzymatic trans-formation at pH 8.0 (middle) and enzymatic transformation at pH 7.4 (bottom). The reactions were performed as described for the *anti*-Markovnikov redox hydrations with the following changes: NADH was used in equimolar concentration to the substrate (5 mM) in the absence of alcohol dehydrogenase to prevent aldehyde reduction. The reactions were stopped after 10 minutes to avoid racemization of the stereocenter in the buffered solution. The reactions at pH 7.4 revealed a higher enantioselectivity, most likely due to reduced racemization.

Fig. S10 Potential enzymatic platform for *anti*-Markovnikov functionalization of alkenes.

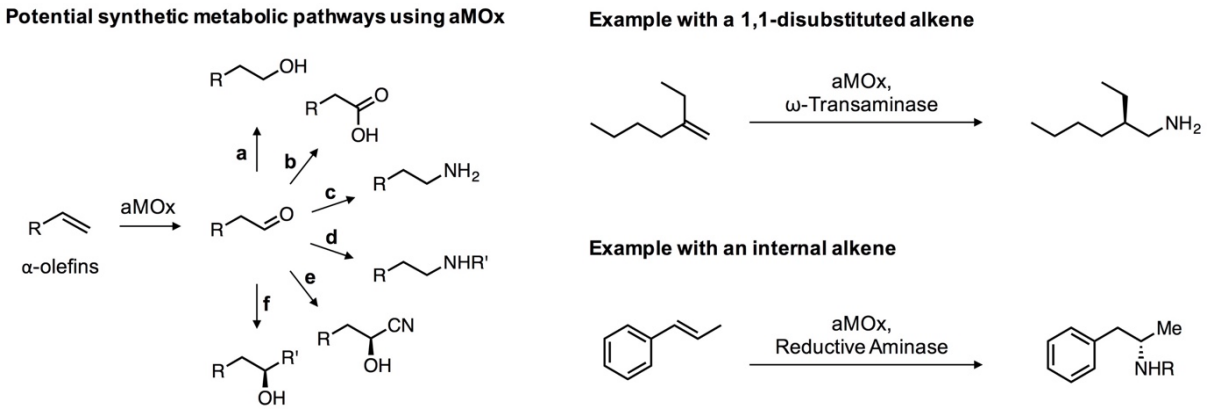

The *anti*-Markovnikov oxygenase (aMOx) can be viewed as the key enzyme in an enzymatic or microbial platform for various challenging *anti*-Markovnikov functionalization reactions (*3*). We have demonstrated that aMOx can be combined with alcohol dehydrogenases to catalyze *anti*-Markovnikov redox hydrations. Since carbonyl compounds are substrates for many biocatalysts, various *anti*-Markovnikov functionalization reactions of alkenes can be envisioned by constructing synthetic metabolic pathways or *de novo* multi-enzyme cascades (*27*, *69*). (**a**) alcohol dehydrogenases (*70*); (**b**) aldehyde dehydrogenases or aldehyde oxidases (*71*, *72*); (**c**) ω-transaminases or imine reductases (*35*, *73*); (**d**) imine reductases, reductive aminase or pictet spenglerases (*73*–*75*); (**e**) hydroxynitril lyases (*76*); (**f**) aldolase or ThDP-dependent lyases (*77*, *78*).

Fig. S11 Examples of additional substrates tested for *anti*-Markovnikov redox hydration using aMOx and an alcohol dehydrogenase.

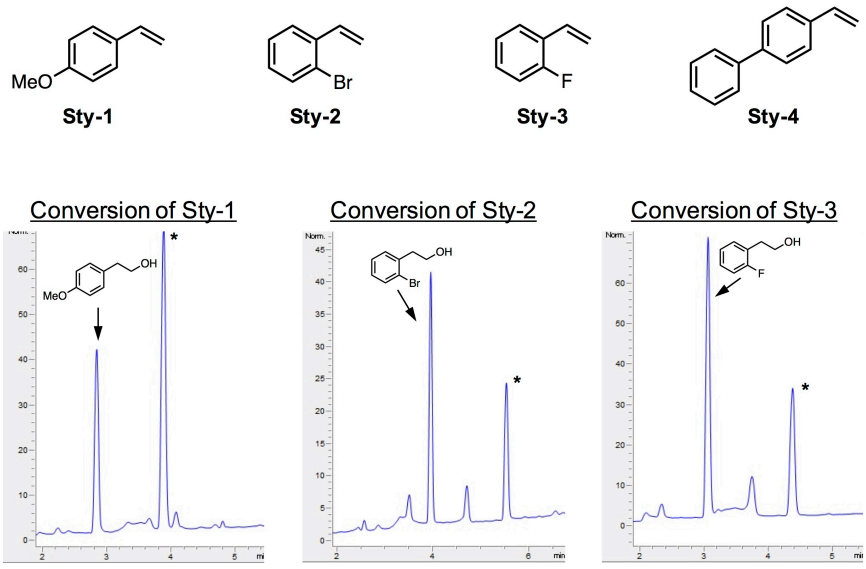

The *anti*-Markovnikov redox hydration of the styrenes **Sty-1-3** showed product formation with low to moderate selectivity for the primary alcohol (see HPLC chromatograms). The peaks labeled with asterisk correspond most likely to the epoxide oxidation product. No product formation could be observed with **Sty-4** as substrate. The reactions were performed using our standard conditions (see section F in general procedures). Because aMOx is fully genetically encoded, the catalyst can be readily optimized by further directed evolution to expand the substrate scope.

IV. Supporting Tables S1 to S3

Table S1 Summary of known catalytic examples for direct and sequential *anti*-Markovnikov oxidation of alkenes.

Type	Alkene	Terminal oxidant	Catalyst	Total turnover numbers	Selectivity† in %	Reference
Modified Wacker oxidation	Styrene	$H_4[PMo_{11}VO_{40}]$ 1.2 equiv.	**$PdCl_2$** 12 mol%	<10	86	(*57*)
	Phtalimide protected allylic amines ‡	O_2*	**$Pd(MeCN)_2Cl(NO_2)$** 5 mol% **$CuCl_2$** 20 mol%	<20	94-100	(*58*)
	Allylic esters ‡	*p*-benzoquinone 1.0 equiv.	**$PdCl_2(PhCN)_2$** 0.5-2.5 mol%	40-140	88-95	(*59*)
	Allylic amides ‡	*p*-benzoquinone 1.0 equiv.	**$PdCl_2(MeCN)_2$** 5 mol%	<20	88-99	(*60*)
	Styrenes	*p*-benzoquinone 1.15 equiv.	**$PdCl_2(MeCN)_2$** 2.5 mol% ***t*-BuOH**	<40	96-100	(*29*, *49*)
	Aliphatic alkenes	O_2*	**$PdCl_2(PhCN)_2$** 5-12 mol% **$CuCl_2$** 5-12 mol% **$AgNO_2$ or $NaNO_2$** 5-6 mol%	<20	50-96	(*50–53*)
	Styrenes	O_2*	**$PdCl_2(MeCN)_2$** 10 mol% **2,5-Pyrroledione** 10 mol%	<10	85-100	(*54*)
Epoxidation-isomerization reaction	Styrenes	2,6-dichloropyridine *N*-oxide 1.03 equiv.	**Ru(IV)-porphyrin** 1-2 mol%	<100	--	(*55*)
	Styrenes	O_2*	**Ru(IV)-porphyrin** 0.5-2 mol%	35-198	--	(*56*)
	Styrenes and aliphatic alkenes	Iodosylbenzene 1.1 equiv.	**Fe(III)-porphyrin** 2 mol%	22-47	--	(*61*)
	Styrenes and aliphatic alkenes	Iodosylbenzene 1.5 equiv.	**$Fe(BF_4)_2$*6H_2O** 2 mol% **pyridine-2,6-dicarboxylic acid** 2 mol%	19-48	--	(*62*)
Dehydrogenative oxygenation	*β*-alkyl styrenes	H_2O	**9-mesityl-10-methylacridinium perchlorate** 5 mol% **$Co(dmgH)_2PyCl$** 3 mol%	6-20	--	(*63*)

*Aerobic *anti*-Markovnikov oxidation of alkenes depend on precious Pd/Ru catalysts.
† *anti*-Markovnikov selectivity (in comparison to Markovnikov selectivity).
‡ Substrate controlled *anti*-Markovnikov selectivity.

Table S2 Summary of directed evolution for alkene *anti*-Markovnikov oxidation.

Round	Parent	Library	Mutations identified
1	$P450_{LA1}$ wild type	Random mutagenesis of the heme domain 2 mutations / 1000 bp	N201K, Y385H, T121A, I198M
2	$P450_{LA1}$ wild type	Recombination of hits identified in round 1	N201K, Y385H, T121A
3	N201K, Y385H, T121A	Random mutagenesis of the heme domain 3.5 mutations / 1000 bp	N209S
4	N201K, Y385H, T121A, N209S	Random mutagenesis of the heme domain 2.5 mutations / 1000 bp	E418G
5	N201K, Y385H, T121A, N209S, E418G	Site-saturation mutagenesis A121X, V123IX, H206X, I326X, W329X, F429X	V123I, I326V
6	N201K, Y385H, T121A, N209S, E418G, V123I, I326V	Site-saturation mutagenesis M118X, S207X, A275X, V278X	M118L
7	N201K, Y385H, T121A, N209S, E418G, V123I, I326V, M118L,	Site-saturation mutagenesis A117X, N119X, R120X, M122X, N124X, S325X	R120H
8	N201K, Y385H, T121A, N209S, E418G, V123I, I326V, M118L, R120H, V327M	Site-saturation mutagenesis Y116X, V327X, R330X, S428X	V327M
9	N201K, Y385H, T121A, N209S, E418G, V123I, I326V, M118L, R120H, V327M	Site-saturation mutagenesis L97X, A103X	A103L
10A	N201K, Y385H, T121A, N209S, E418G, V123I, I326V	Site-saturation mutagenesis F383X, G384X, H385X, G386X, S387X, H388X, Q389X, M391X, G392X, K393X	H385V, G386A, S387Y, Q389N, M391L
10B	N201K, Y385H, T121A, N209S, E418G, V123I, I326V, M118L, R120H, V327M, A103L	Combination of mutations identified in 10A into final variant of round 9	H385V, M391L

Table S3 Activity of P450 variants generated by directed evolution for the *anti*-Markovnikov oxidation of styrene.

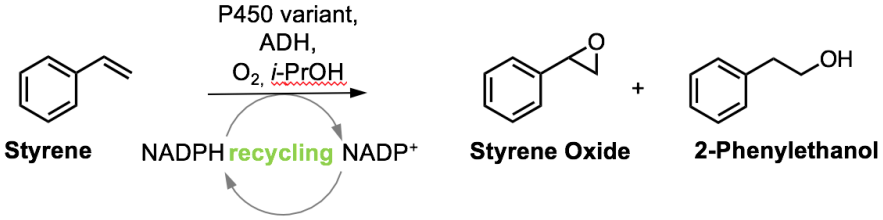

Round	Variant	TON ± SD	*Anti*-Markovnikov selectivity (calc. as % alcohol product)
Parent	$P450_{LA1}$ wild type	99 ± 5	45
1A	N201K, Y385H	190 ± 0	45
1B	T121A, I198M	390 ± 15	55
2	N201K, Y385H, T121A	520 ± 2	55
3	N201K, Y385H, T121A, N209S	750 ± 7	55
4 (= P7)	N201K, Y385H, T121A, N209S, E418G	1200 ± 50	54
5	N201K, Y385H, T121A, N209S, E418G, V123I, I326V	1600 ± 167	62
6	N201K, Y385H, T121A, N209S, E418G, V123I, I326V, M118L	1800 ± 24	68
7	N201K, Y385H, T121A, N209S, E418G, V123I, I326V, M118L, R120H	2500 ± 51	72
8	N201K, Y385H, T121A, N209S, E418G, V123I, I326V, M118L, R120H, V327M	3500 ± 126	76
9	N201K, Y385H, T121A, N209S, E418G, V123I, I326V, M118L, R120H, V327M, A103L	3700 ± 78	78
10 (aMOx)	N201K, T121A, N209S, E418G, V123I, I326V, M118L, R120H, V327M, A103L, M391L, H385V	3800 ± 99	81

- Round 1 to 4 are based on colorimetric screening of random mutagenesis libraries of the heme domain using the Purpald assay.
- Round 5 to 10 are based on HPLC screening of libraries generated by site-saturation mutagenesis.

V. NMR spectra of the isotopic labeling experiment

(**a**) ^{1}H NMR spectra comparison of 2-phenylethanol (standard) and 2-phenylethanol-1,2-d_2. (product of the enzymatic conversion).

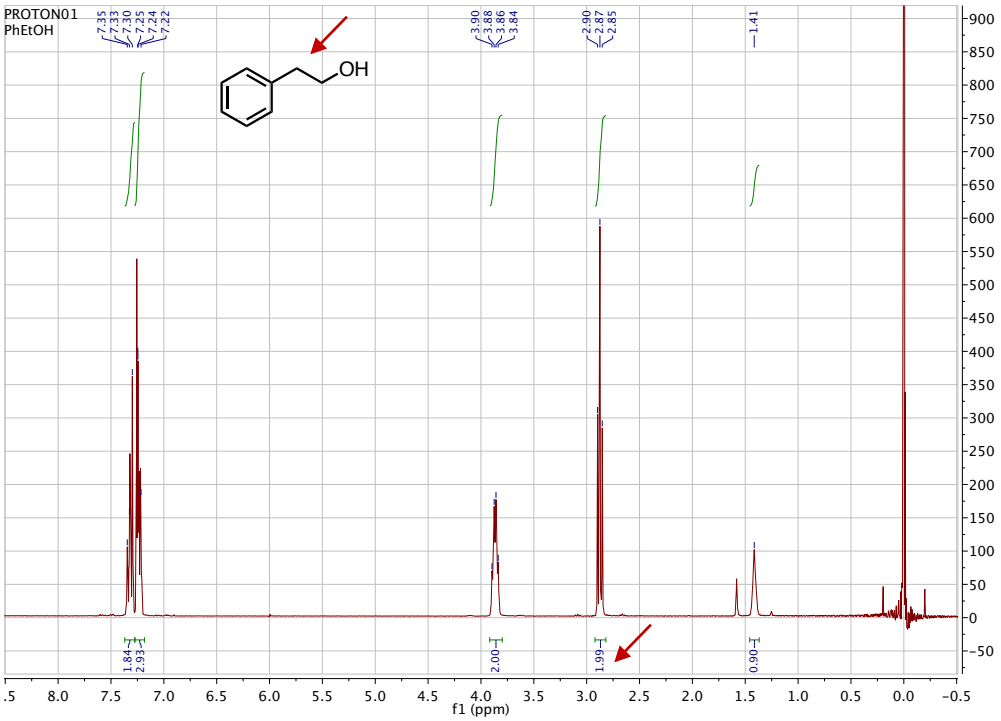

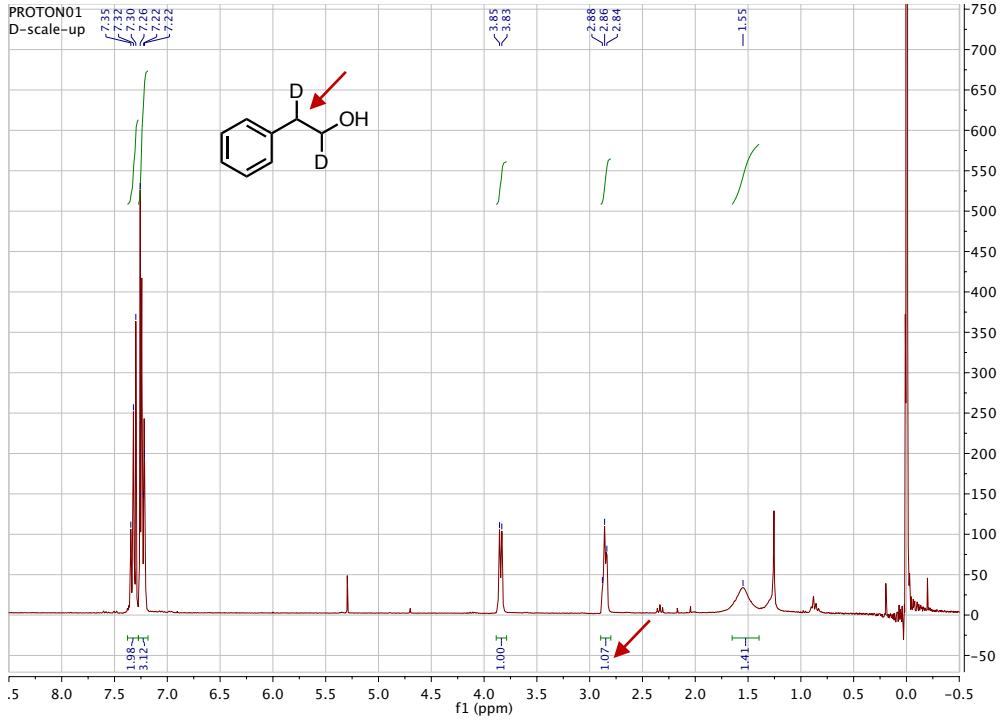

(**b**) ^{13}C NMR spectra comparison of 2-phenylethanol (standard) and 2-phenylethanol-1,2-d_2. (product of the enzymatic conversion).

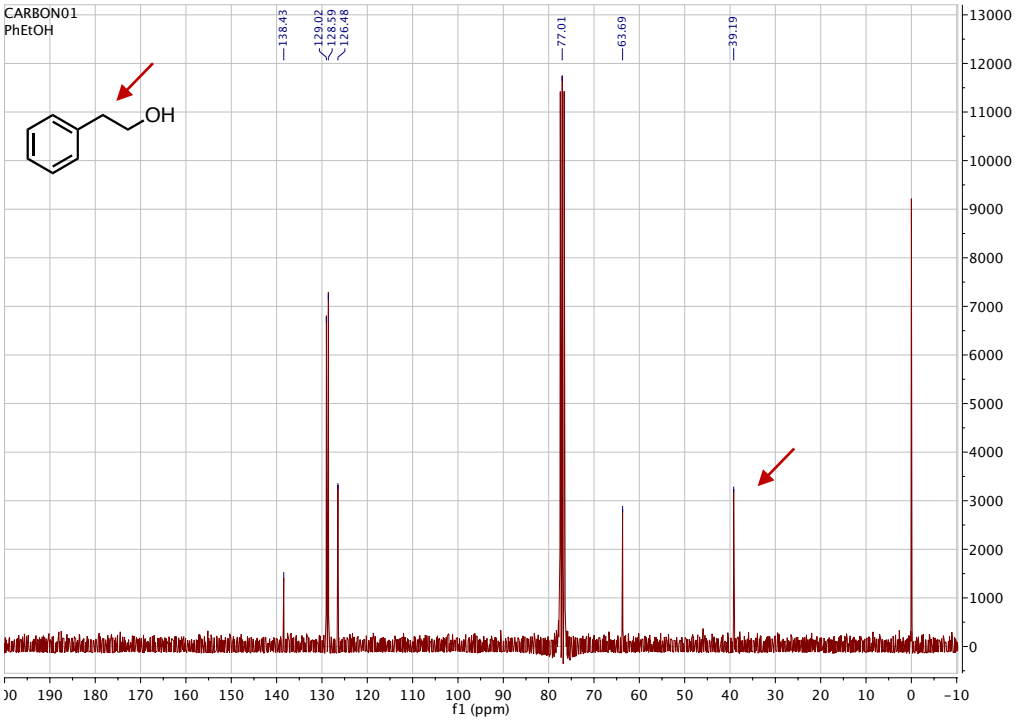

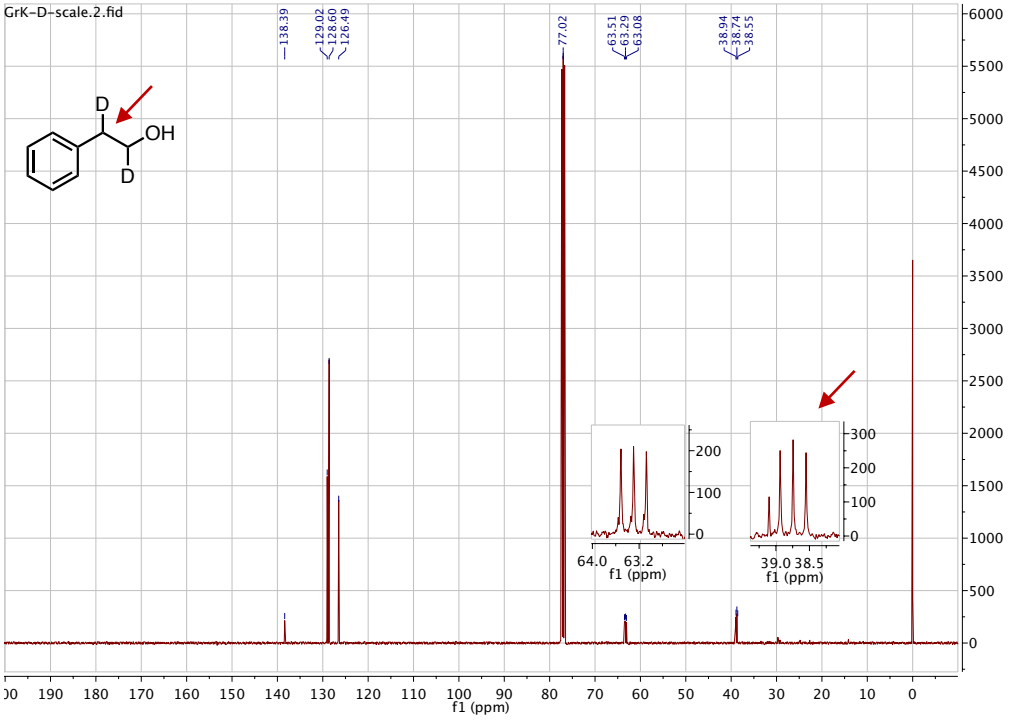

VI. Preparative scale reactions

General protocol. To optimize the system for high conversion, we worked with a reduced substrate loading (2 mM final concentration) that enabled efficient cofactor recycling with the current setup. Purified aMOx (1.0 µM final conc., 0.05 mol% catalyst) was mixed in a flask with $NADP^+$ (0.4 mM final conc., 0.2 equivalents), alcohol dehydrogenase (10 U/mL, Sigma Aldrich, 49641) and alkene (2 mM final conc., 100 mM stock solution in 1:1 DMSO and isopropanol) in a phosphate buffer system (100 mM sodium phosphate, pH 8.0, 150 mM NaCl, 2.0% glycerol). Preparative scale reactions were performed with 40 and 60 mg starting material (0.23 – 0.50 mmol scale). The reactions were carried out in 500 mL flasks by incubating the mixture for 2 h at room temperature (120 rpm). The reaction was extracted with ethyl acetate/hexanes 4:1 (three times, 100 mL, 50 mL and 35 mL). The combined organic layers were washed with water (20 mL) and brine (20 mL), dried over $MgSO_4$, filtered, concentrated, and purified by column chromatography.

2-(4-Chlorophenyl)ethanol (8): The reaction was performed on 0.25-mmol scale. The product was purified by column chromatography (9 – 20% ethyl acetate/hexanes). Isolated 35.9 mg (82% yield, 1600 TTN). ^{1}H NMR (300 MHz, $CDCl_3$): δ 7.30–7.26 (m, 2H), 7.17–7.14 (m, 2H), 3.83 (t, *J* = 6.5 Hz, 2H), 2.83 (t, *J* = 6.5 Hz, 2H), 1.66 (s, 1H); ^{13}C NMR (75 MHz, $CDCl_3$): δ 137.14, 132.38, 130.47, 128.76, 63.56, 38.57.

2-[4-(Trifluoromethyl)phenyl]ethanol (9): The reaction was performed on 0.23-mmol scale. The product was purified by column chromatography (9 – 20% ethyl acetate/hexanes). Isolated 31.3 mg (73% yield, 1500 TTN). ^{1}H NMR (300 MHz, $CDCl_3$): δ 7.57 (d, *J* = 8.1 Hz, 2H), 7.35 (d, *J* = 8.1 Hz, 2H), 3.89 (t, *J* = 6.5 Hz, 2H), 2.93 (t, *J* = 6.5 Hz, 2H), 1.59 (s, 1H); ^{13}C NMR (101 MHz, $CDCl_3$): δ 142.96 (q, *J* = 1.2 Hz), 129.48, 128.95 (q, *J* = 32.4 Hz), 125.56 (q, *J* = 3.8 Hz), 124.45 (q, *J* = 271.9 Hz), 63.38, 39.05; ^{19}F NMR (282 MHz, $CDCl_3$): δ -62.45.

(*S*)-1-Phenyl-2-propanol (16): The reaction was performed on 0.50-mmol scale. The product was purified by column chromatography (9 – 20% ethyl acetate/hexanes). Isolated 19.1 mg (28% yield, 560 TTN, >99:1 er). ^{1}H NMR (300 MHz, $CDCl_3$): δ 7.35–7.20 (m, 5H), 4.07–3.98 (m, 1H), 2.80 (dd, *J* = 13,4, 4,9 Hz, 1H), 2.69 (dd, *J* = 13,4, 7,9 Hz, 1H), 1.59 (s, 1H), 1.25 (d, *J* = 6.2 Hz, 3H); ^{13}C NMR (75 MHz, $CDCl_3$): δ 138.62, 129.52, 128.68, 126.62, 69.02, 45.92, 22.93.

VII. NMR spectra for preparative scale reactions

^{1}H NMR: 2-(4-chlorophenyl)ethanol (**8**)

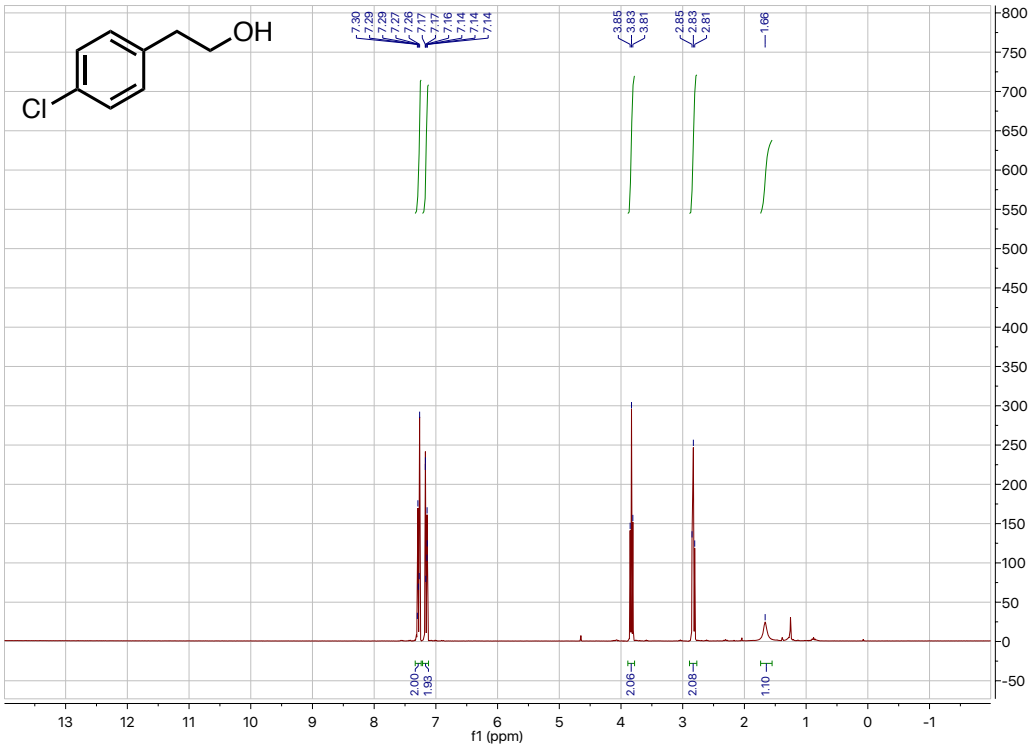

^{13}C NMR: 2-(4-chlorophenyl)ethanol (**8**)

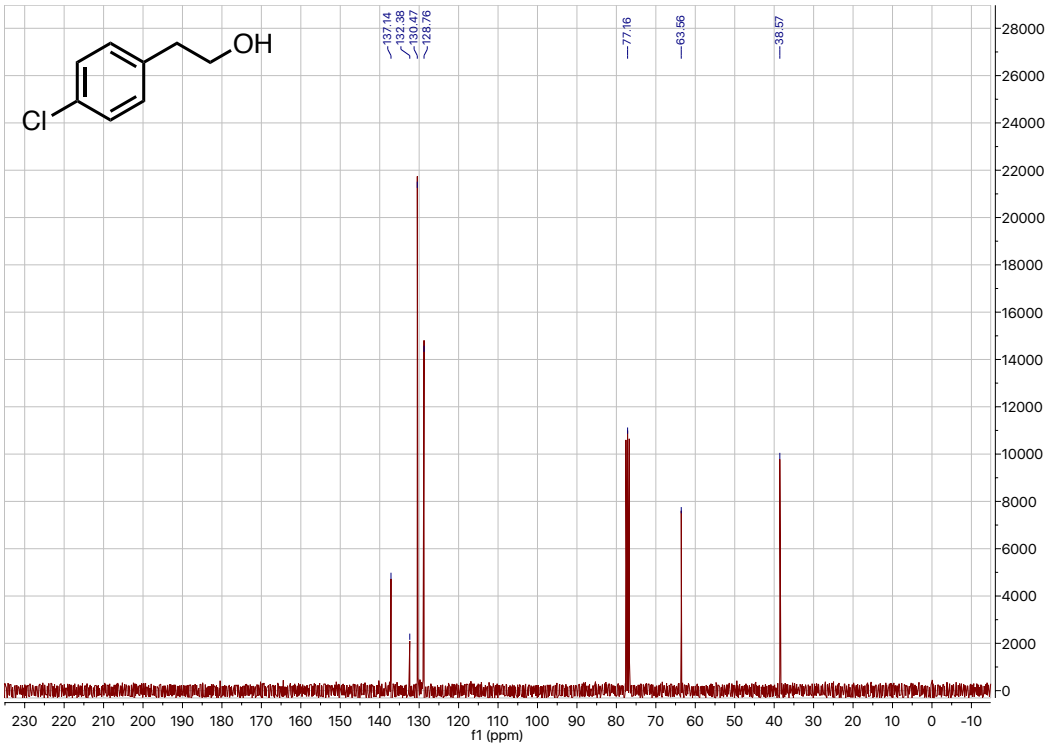

^{1}H NMR: 2-[4-(trifluoromethyl)phenyl]ethanol (**9**)

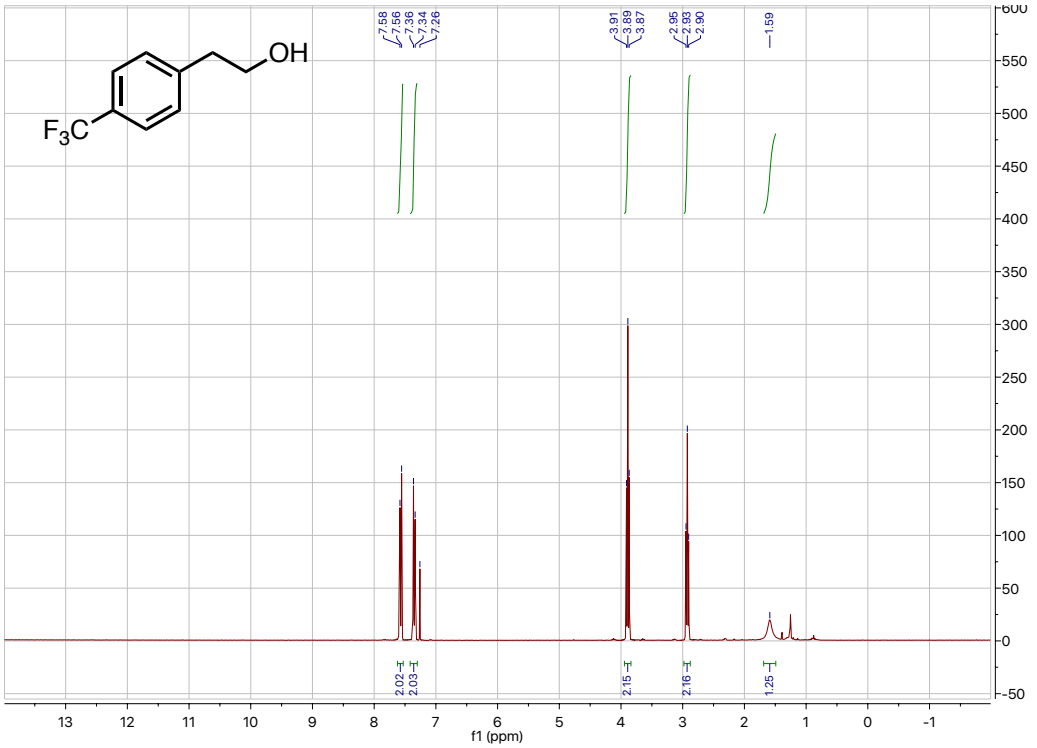

^{13}C NMR: 2-[4-(trifluoromethyl)phenyl]ethanol (**9**)

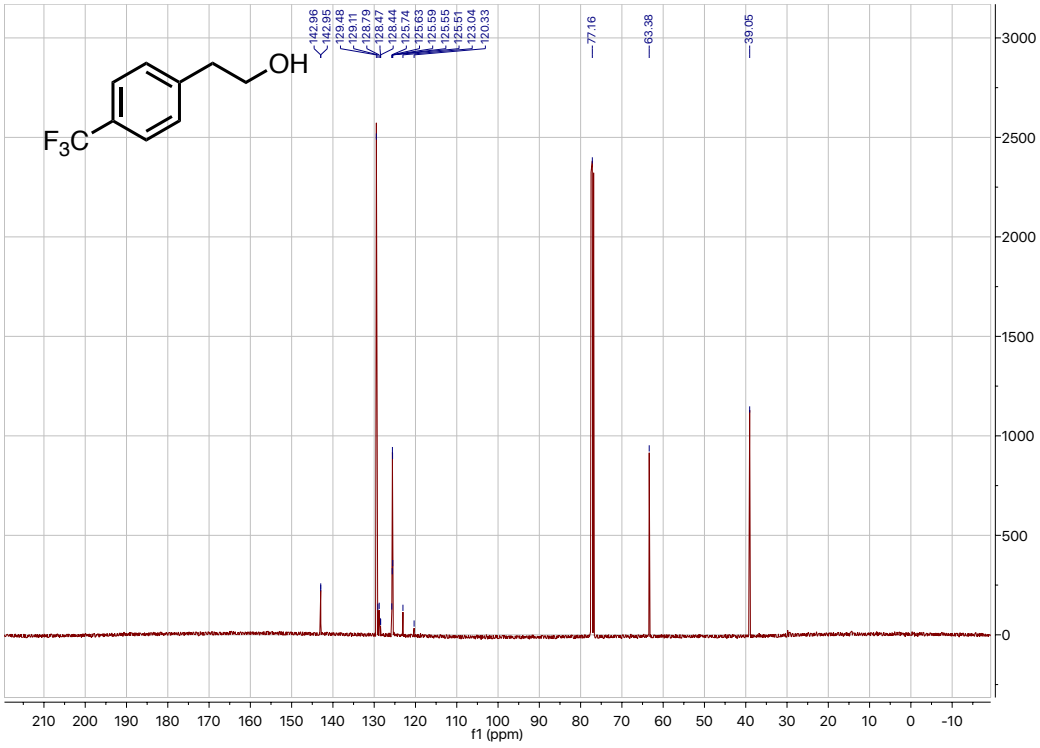

^{19}F NMR: 2-[4-(trifluoromethyl)phenyl]ethanol (**9**)

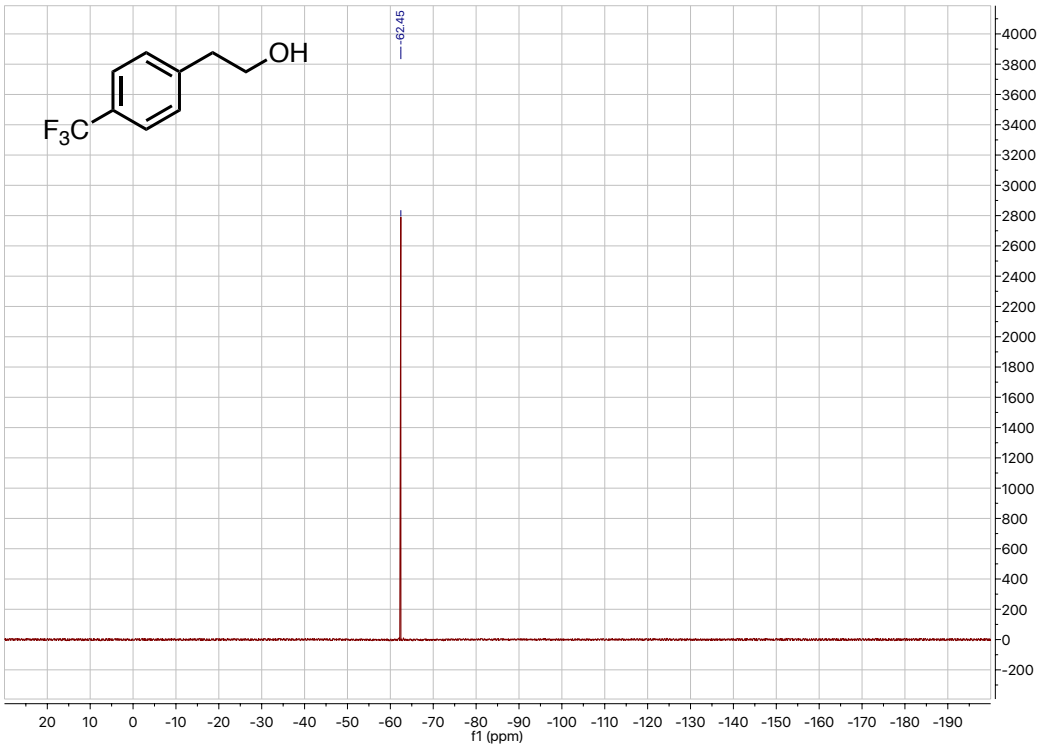

^{1}H NMR: (*S*)-1-phenyl-2-propanol (**16**)

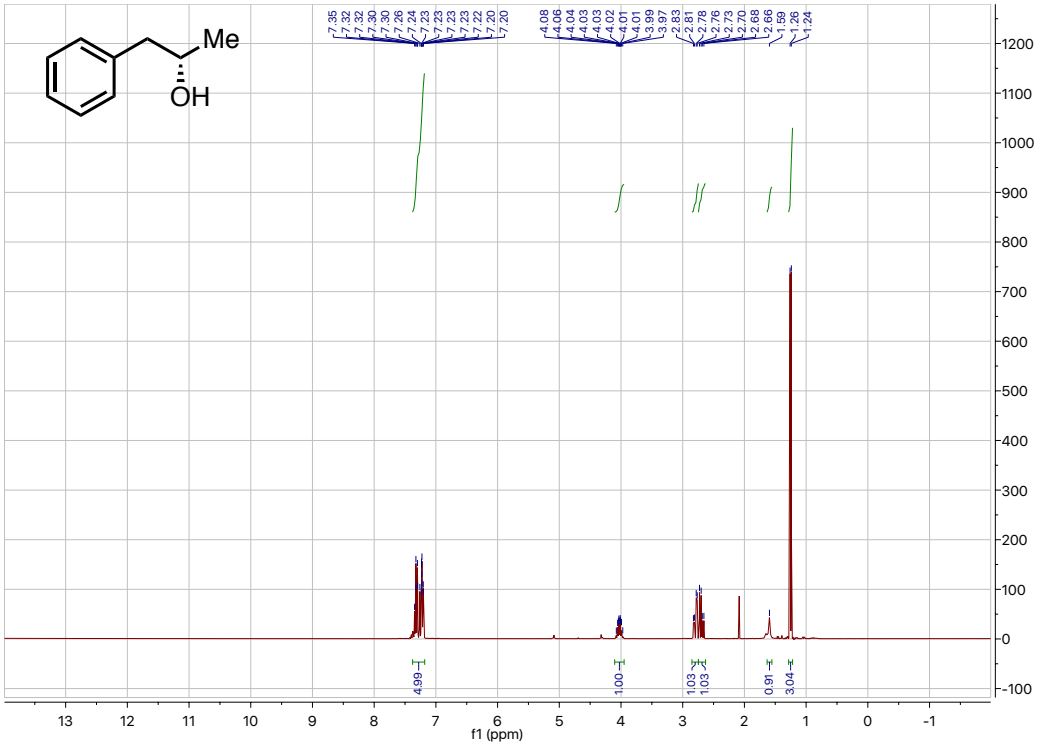

^{13}C NMR: (*S*)-1-phenyl-2-propanol (**16**)

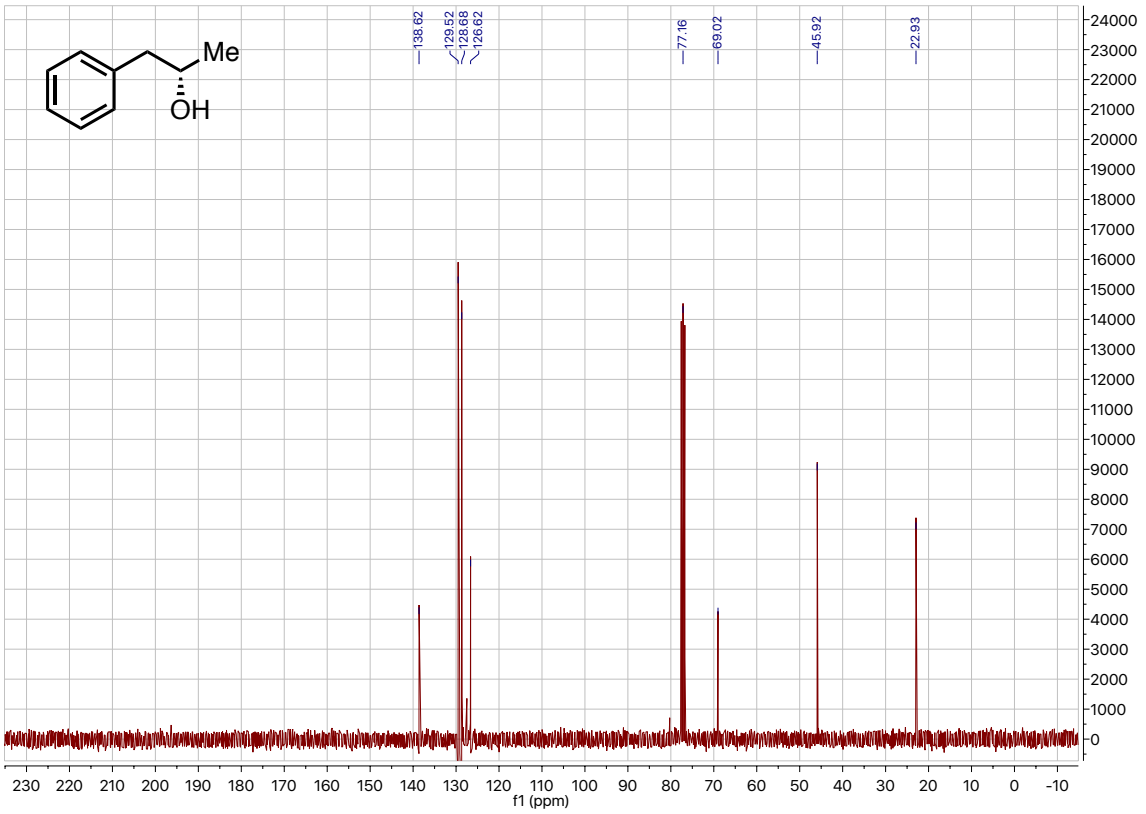

VIII. HPLC calibration curves

(**a**) **HPLC calibration**: External standard calibration curves were created for quantitative HPLC analysis using commercial standards.

(**b**) Calibration curves for styrene, 2-phenylethanol and styrene oxide at 210 nm.

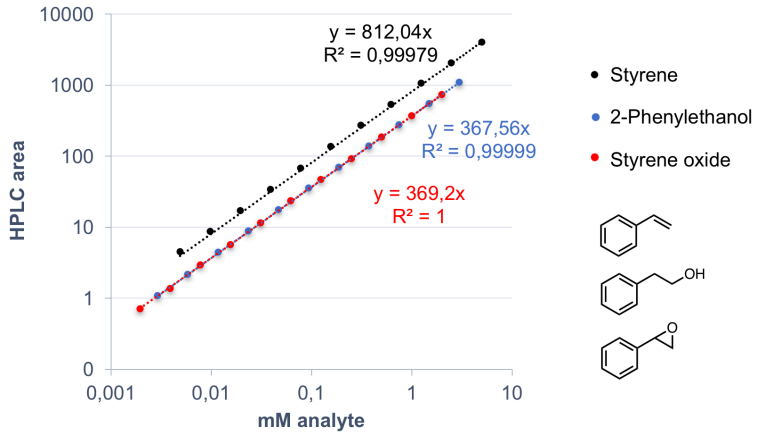

(**c**) Calibration curves for 4-chlorostyrene, 2-(4-chlorophenyl)ethanol and 2-(4-chlorophenyl)oxirane at 210 nm.

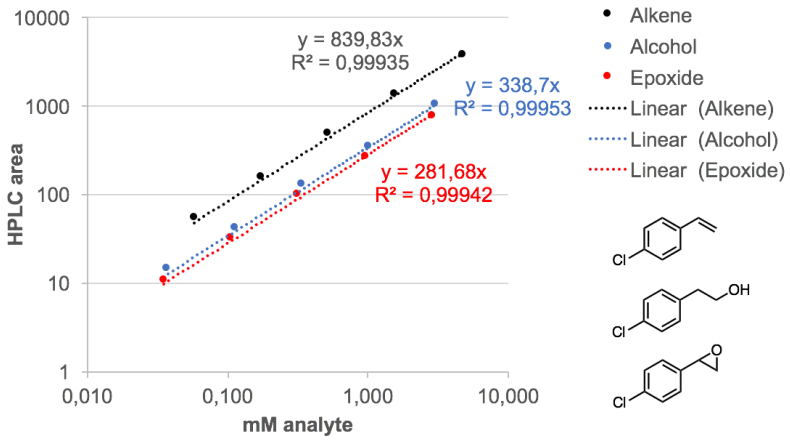

(**d**) Calibration curves for 4-(trifluoromethyl)styrene, 2-[4-(trifluoromethyl)phenyl]ethanol and 2-[4-(trifluoromethyl)phenyl]oxirane at 210 nm.

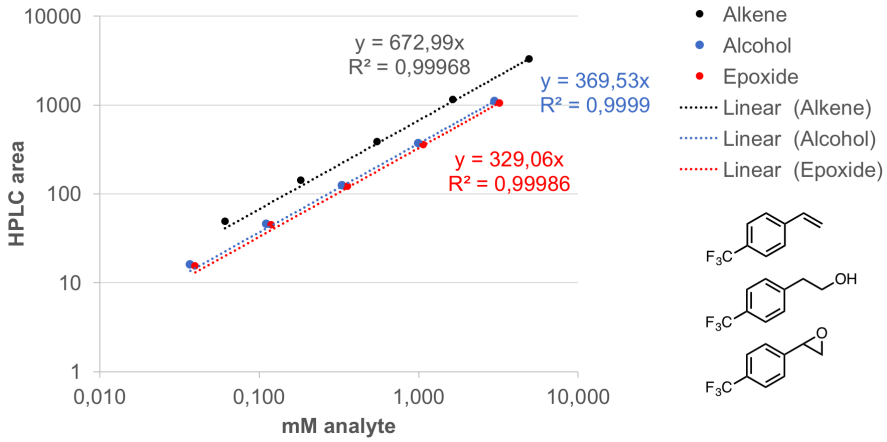

(**e**) Calibration curves for 3-chlorostyrene, 2-(3-chlorophenyl)ethanol and 2-(3-chlorophenyl)oxirane at 210 nm.

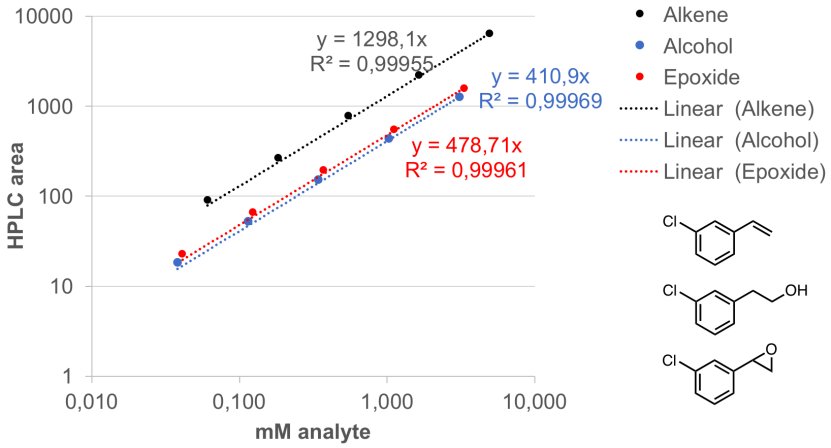

(**f**) Calibration curves for 4-methylstyrene, 2-(4-methylphenyl)ethanol and 2-(4-methylphenyl)oxirane at 210 nm.

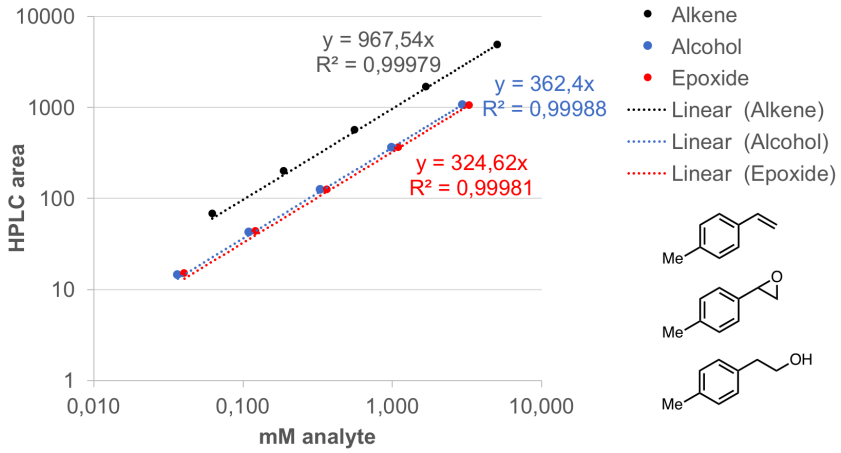

(**g**) Calibration curves for 4-bromostyrene, 2-(4-bromophenyl)ethanol and 2-(4-bromophenyl)oxirane at 210 nm.

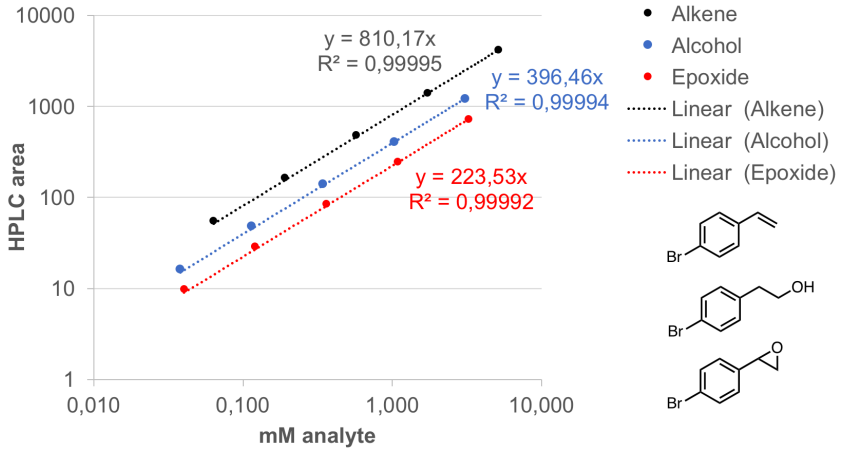

(**h**) Calibration curves for 3-(trifluoromethyl)styrene, 2-[3-(trifluoromethyl)phenyl]ethanol and 2-[3-(trifluoromethyl)phenyl]oxirane at 210 nm.

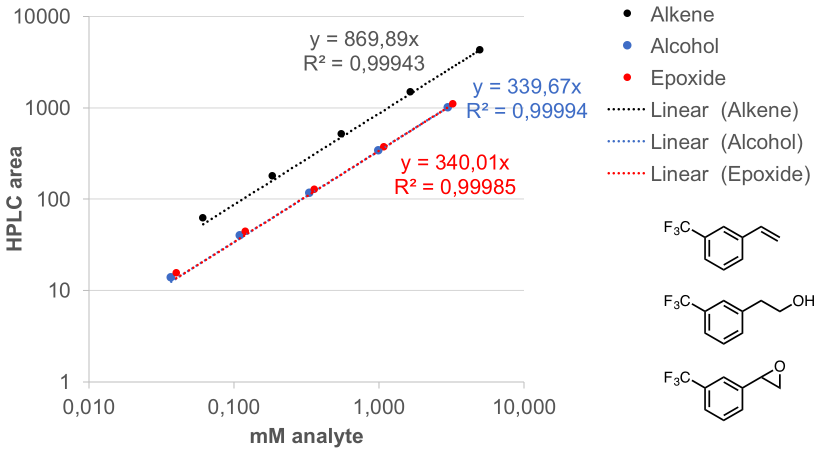

(**i**) Calibration curves for 2-(trifluoromethyl)styrene, 2-[2-(trifluoromethyl)phenyl]ethanol and 2-[2-(trifluoromethyl)phenyl]oxirane at 210 nm.

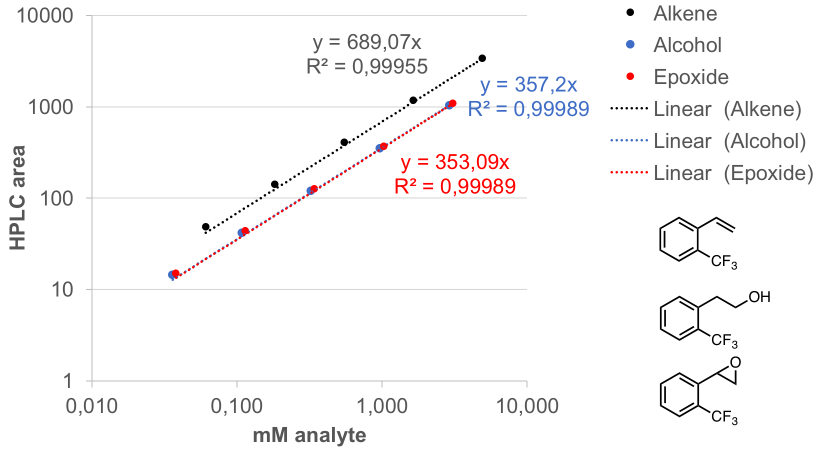

(**j**) Calibration curves for α-methylstyrene, 2-phenyl-1-propanol and 2-methyl-2-phenyloxirane at 210 nm.

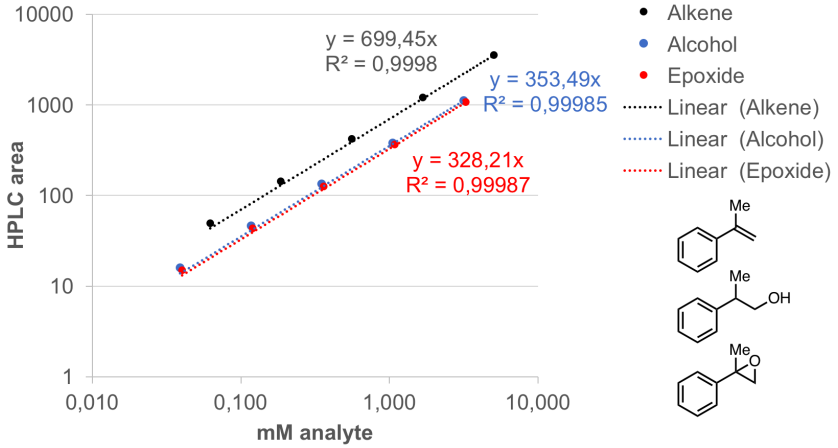

(**k**) Calibration curves for *trans*-β-methylstyrene, 1-phenyl-2-propanol and *trans*-2-methyl-3-phenyloxirane at 210 nm.

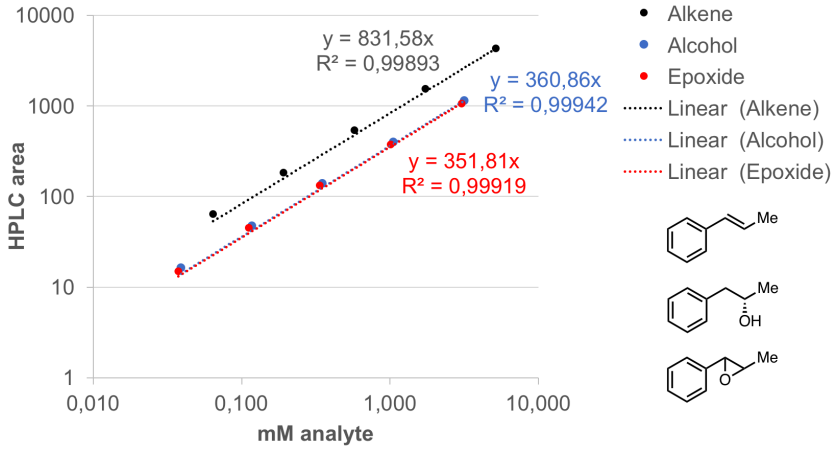

IX. HPLC traces for *anti*-Markovnikov redox hydration

(**a**) Product identities were confirmed by retention time and additionally by HPLC co-injections of reaction mixtures with standard molecules. The recovery of the starting material was calculated for each run and was between 92.5 and 106.9%. The average recovery was 98.7%. The reactions are not optimized for conversion at this stage. Depending on the substrate, conversions of 5.5 to 45% were achieved in these proof-of- concept biocatalytic *anti*-Markovnikov redox hydrations. Representative HPLC traces are shown below.

(**b**) Product ratio as analyzed by HPLC for the *anti*-Markovnikov redox hydration of 4-chlorostyrene measured at 210 nm.

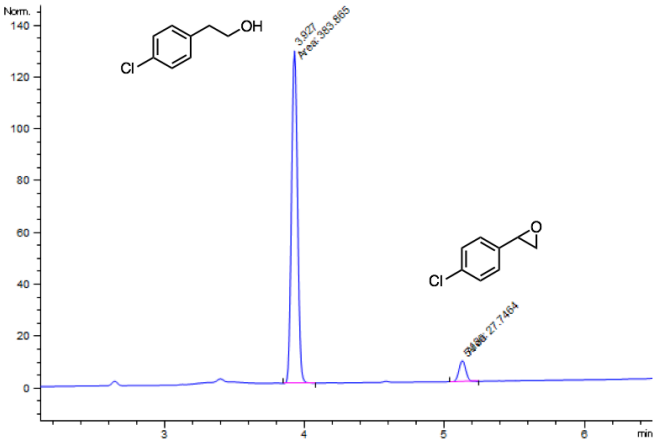

(**c**) Product ratio as analyzed by HPLC for the *anti*-Markovnikov redox hydration of 4-(trifluoromethyl)styrene measured at 210 nm.

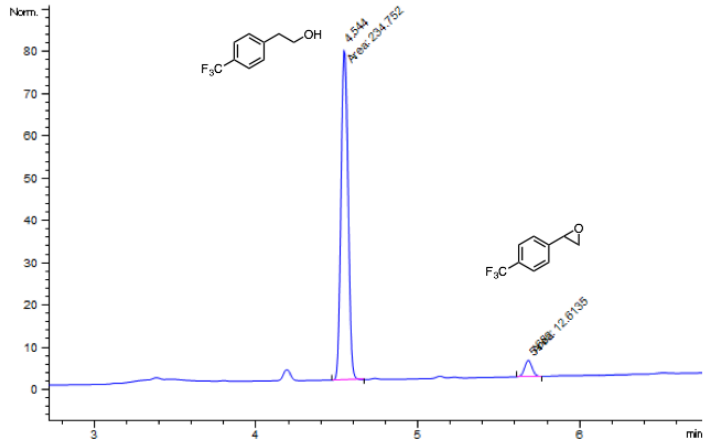

(**d**) Product ratio as analyzed by HPLC for the *anti*-Markovnikov redox hydration of 3-chlorostyrene measured at 210 nm.

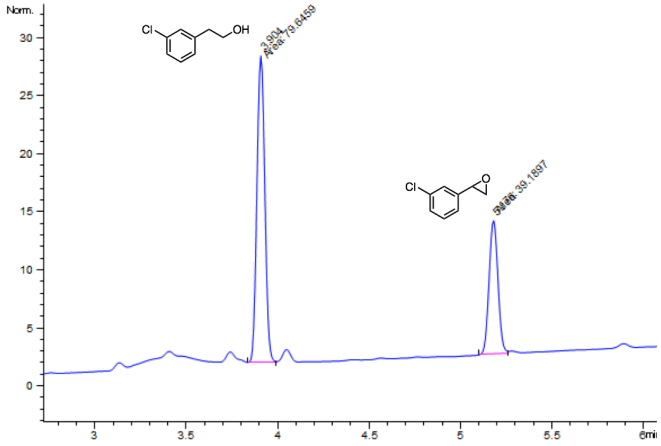

(**e**) Product ratio as analyzed by HPLC for the *anti*-Markovnikov redox hydration of 4-methylstyrene measured at 210 nm.

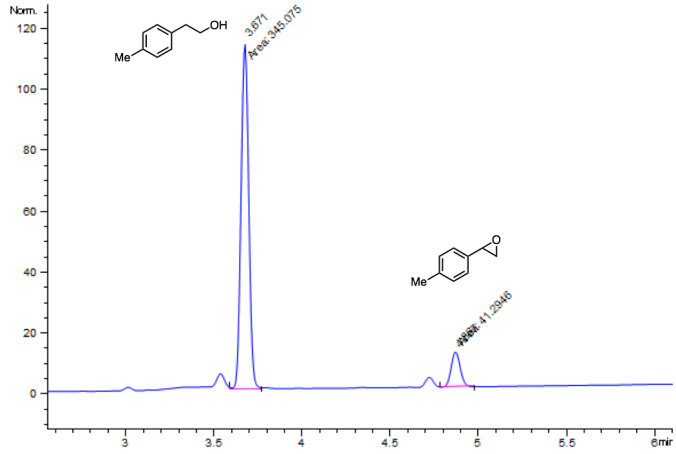

(**f**) Product ratio as analyzed by HPLC for the *anti*-Markovnikov redox hydration of 4-bromostyrene measured at 210 nm.

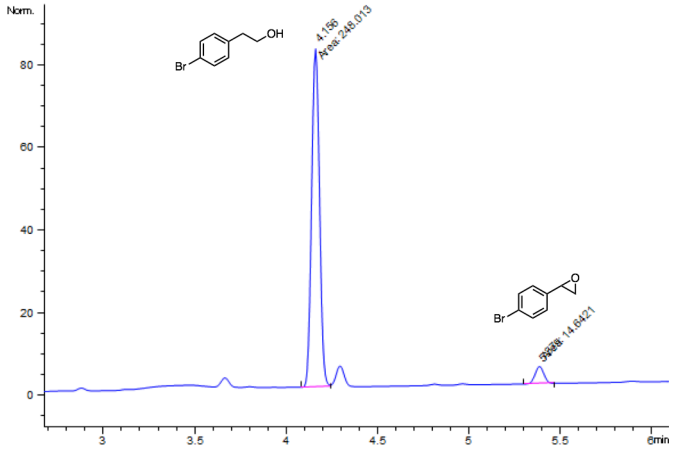

(**g**) Product ratio as analyzed by HPLC for the *anti*-Markovnikov redox hydration of 3-(trifluoromethyl)styrene measured at 210 nm.

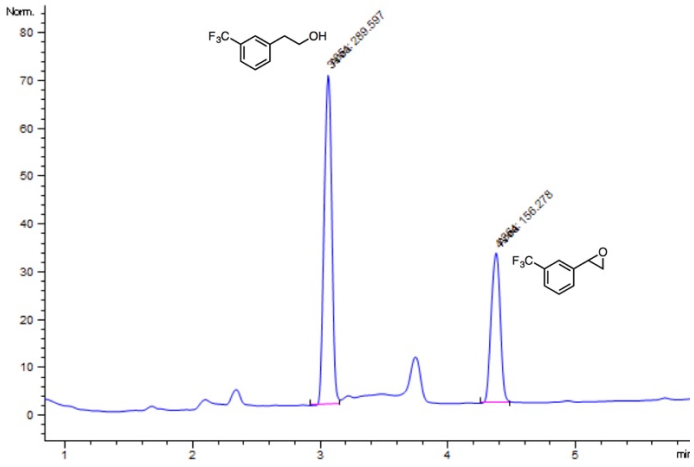

(**h**) Product ratio as analyzed by HPLC for the *anti*-Markovnikov redox hydration of 2-(trifluoromethyl)styrene measured at 210 nm.

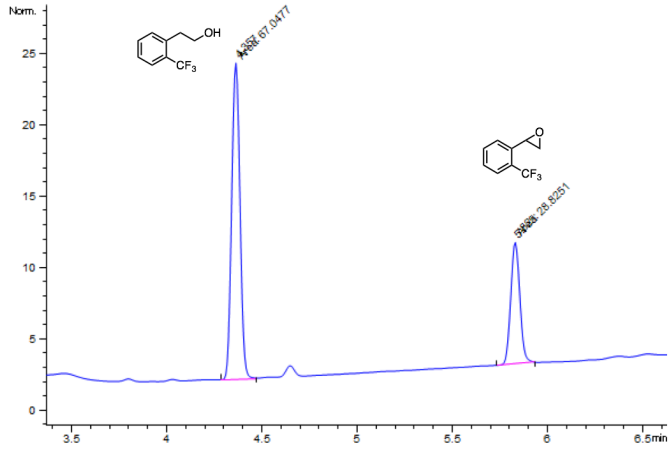

(**i**) Product ratio as analyzed by HPLC for the *anti*-Markovnikov redox hydration of α-methylstyrene measured at 210 nm (the peak at 2.5 min corresponds to the allylic oxidation product, which was generated as a side product).

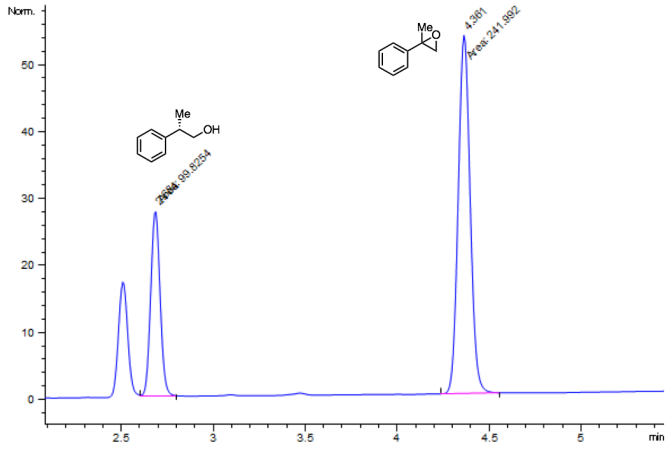

(**j**) Product ratio as analyzed by HPLC for the *anti*-Markovnikov redox hydration of *trans*-β-methylstyrene measured at 210 nm.

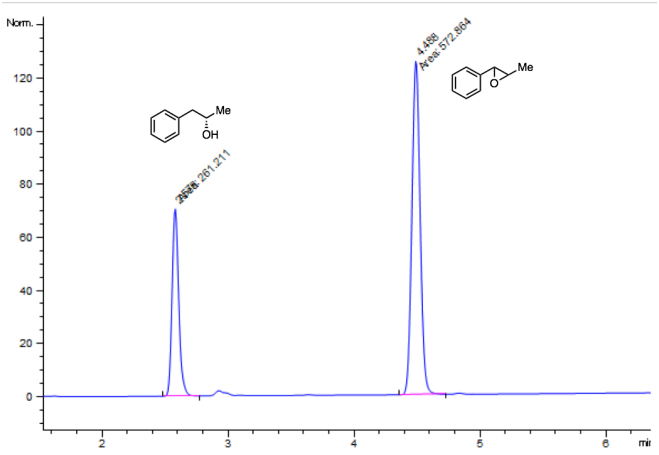

(**k**) Product ratio as analyzed by HPLC for the *anti*-Markovnikov redox hydration of styrene measured at 210 nm.

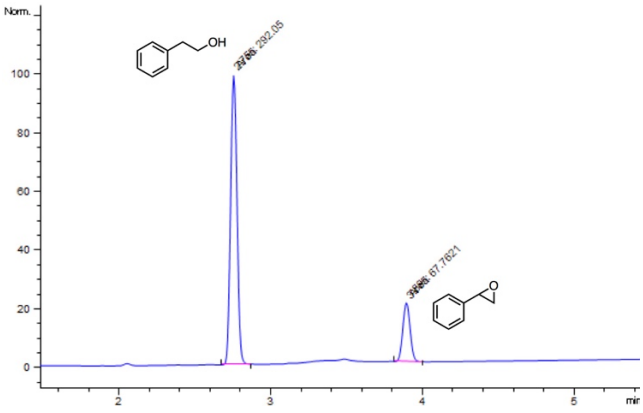

X. Chiral GC analysis for enantioselective *anti*-Markovnikov redox hydration

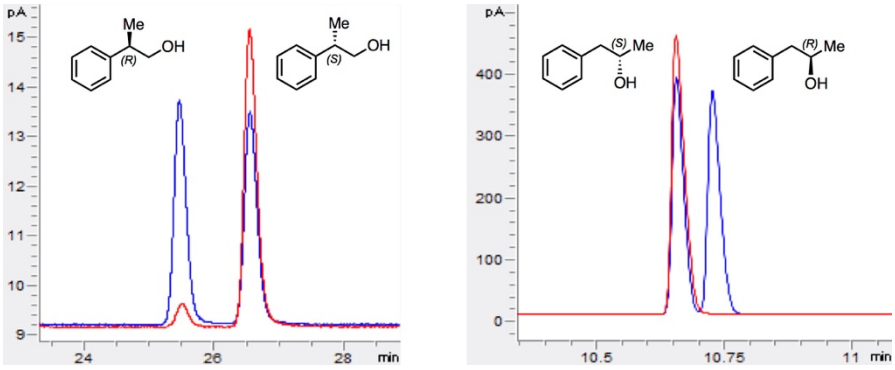

The figures show chiral GC traces for *anti*-Markovnikov redox hydration of α-methylstyrene (left) and β-methylstyrene (right). Each figure shows the products of enzymatic conversion (red) in comparison to the racemic standard (blue).

XI. NMR characterization and spectra of standard compounds

Characterization of reaction products. Authentic standards corresponding to enzymatic reaction products were bought from Sigma or custom synthesized by TCI America. All products are known compounds, and their spectral data are in agreement with reported values.(*79–84*)

2-Phenylethanol: ^{1}H NMR (300 MHz, $CDCl_3$): δ 7.35–7.21 (m, 5H), 3.86 (t, *J* =6.6 Hz, 2H), 2.87 (t, *J* = 6.6 Hz, 2H), 1.54 (s, 1H); ^{13}C NMR (75 MHz, $CDCl_3$): δ 138.60, 129.16, 128.70, 126.59, 63.80, 39.32.

2-(4-chlorophenyl)ethanol (8): ^{1}H NMR (300 MHz, $CDCl_3$): δ 7.30–7.26 (m , 2H), 7.18–7.14 (m, 2H), 3.83 (t, *J* = 6.5 Hz, 2H), 2.83 (t, *J* = 6.6 Hz, 2H), 1.55 (s, 1H); ^{13}C NMR (75 MHz, $CDCl_3$): δ 137.14, 132.38, 130.48, 128.77, 63.56, 38.58.

2-[4-(trifluoromethyl)phenyl]ethanol (9): ^{1}H NMR (300 MHz, $CDCl_3$): δ 7.57 (d, *J* = 8.0 Hz, 2H), 7.35 (d, *J* = 8.0 Hz, 2H), 3.88 (t, *J* = 6.5 Hz, 2H), 2.92 (t, *J* = 6.5 Hz, 2H), 1.56 (s, 1H); ^{13}C NMR (101 MHz, $CDCl_3$): δ 142.96 (q, *J* = 1.2 Hz), 129.47, 128.92 (q, *J* = 32.4 Hz), 125.56 (q, *J* = 3.8 Hz), 124.45 (q, *J* = 273.71 Hz), 63.36, 39.04; ^{19}F NMR (282 MHz, $CDCl_3$): δ -62.45.

2-(3-chlorophenyl)ethanol (10): ^{1}H NMR (300 MHz, $CDCl_3$): δ 7.27–7.19 (m, 3H), 7.13–7.09 (m, 1H), 3.85 (q, *J* = 6.3 Hz, 2H), 2.84 (t, *J* = 6.5 Hz, 2H), 1.54 (t, *J* = 5.5 Hz, 1H); ^{13}C NMR (75 MHz, $CDCl_3$)i: δ 140.79, 134.42, 129.90, 129.24, 127.35, 126.78, 63.43, 38.91.

2-(4-methylphenyl)ethanol (11): ^{1}H NMR (300 MHz, $CDCl_3$): δ 7.13 (s, 4H), 3.84 (q, *J* = 6.3 Hz, 2H), 2.83 (t, *J* = 6.6 Hz, 2H), 2.34 (s, 3H), 1.50 (t, *J* = 5.6 Hz, 1H); ^{13}C NMR (75 MHz, $CDCl_3$): δ 136.13, 135.40, 129.40, 129.03, 63.90, 38.86, 21.15.

2-(4-bromophenyl)ethanol (12): ^{1}H NMR (300 MHz, $CDCl_3$): δ 7.45–7.41 (m, 2H), 7.13–7.08 (m, 2H), 3.83 (q, *J* = 6.4 Hz, 2H), 2.81 (t, *J* = 6.5 Hz, 2H), 1.52 (t, *J* = 5.7 Hz, 1H); ^{13}C NMR (75 MHz, $CDCl_3$): δ 137.68, 131.73, 130.88, 120.43, 63.49, 38.65.

2-[3-(trifluoromethyl)phenyl]ethanol (13): ^{1}H NMR (300 MHz, $CDCl_3$): δ 7.50 – 7.47 (m, 2H), 7.45 – 7.41 (m, 2H), 3.88 (q, *J* = 6.4 Hz, 2H), 2.93 (t, *J* = 6.5 Hz, 2H), 1.56 (t, *J* = 5.6 Hz, 1H); ^{13}C NMR (75 MHz, $CDCl_3$): δ 139.75, 132.59 (q, *J* = 1.5 Hz), 130.96 (q, *J* = 32.1 Hz), 129.05, 125.83 (q, *J* = 3.8 Hz), 123.46 (q, *J* = 3.8 Hz), 122.48, 63.40, 39.01; ^{19}F NMR (282 MHz, $CDCl_3$) δ -62.62.

2-[2-(trifluoromethyl)phenyl]ethanol (14): ^{1}H NMR (300 MHz, $CDCl_3$): δ 7.66–7.64 (m, 1H), 7.51–7.30 (m, 3H), 3.87 (t, *J* = 6.8 Hz, 2H), 3.07 (t, *J* = 6.8 Hz, 2H), 1.61 (s, 1H); ^{13}C NMR (75 MHz, $CDCl_3$): δ 137.04 (q, *J* = 1.7 Hz), 131.81, 131.71, 128.94 (q, *J* = 29.7 Hz), 126,53, 126.16 (q, *J* = 5.8 Hz), 124.54 (q, *J* = 273.7 Hz), 63.27, 35,93; ^{19}F NMR (282 MHz, $CDCl_3$) δ -59.44.

2-phenyl-1-propanol (15): ^{1}H NMR (300 MHz, $CDCl_3$): δ 7.37–7.21 (m, 5H), 3.70 (d, *J* = 6.8 Hz, 2H), 2.95 (q, *J* = 6.9 Hz, 1H), 1.47 (s, 1H), 1.28 (d, *J* = 7.0 Hz, 3H). ^{13}C NMR (75 MHz, $CDCl_3$): δ 143.77, 128.76, 127.61, 126.80, 68.84, 42.56, 17.71.

1-phenyl-2-propanol (16): ^{1}H NMR (300 MHz, $CDCl_3$): δ 7.35–7.20 (m, 5H), 4.07–3.98 (m, 1H), 2.80 (dd, *J* = 13,4, 4,9 Hz, 1H), 2.69 (dd, *J* = 13,4, 7,9 Hz, 1H), 1.59 (s, 1H), 1.25 (d, *J* = 6.2 Hz, 3H); ^{13}C NMR (75 MHz, $CDCl_3$): δ 138.62, 129.52, 128.68, 126.62, 69.01, 45.92, 22.92.

^{1}H NMR 2-Phenylethanol

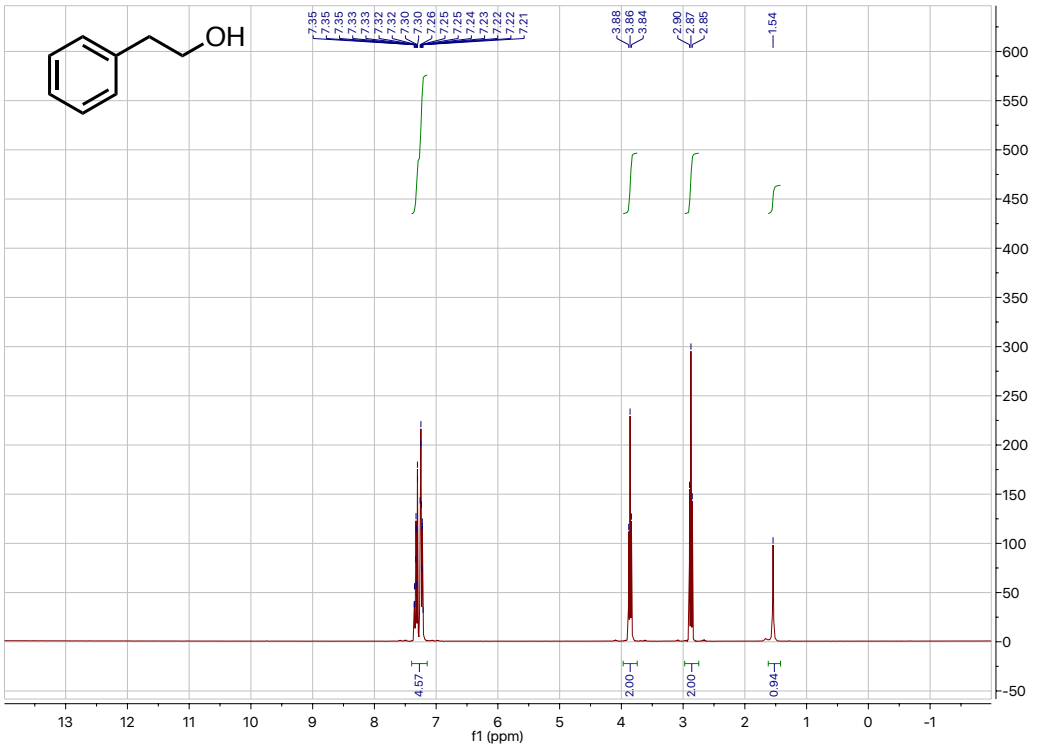

^{13}C NMR 2-Phenylethanol

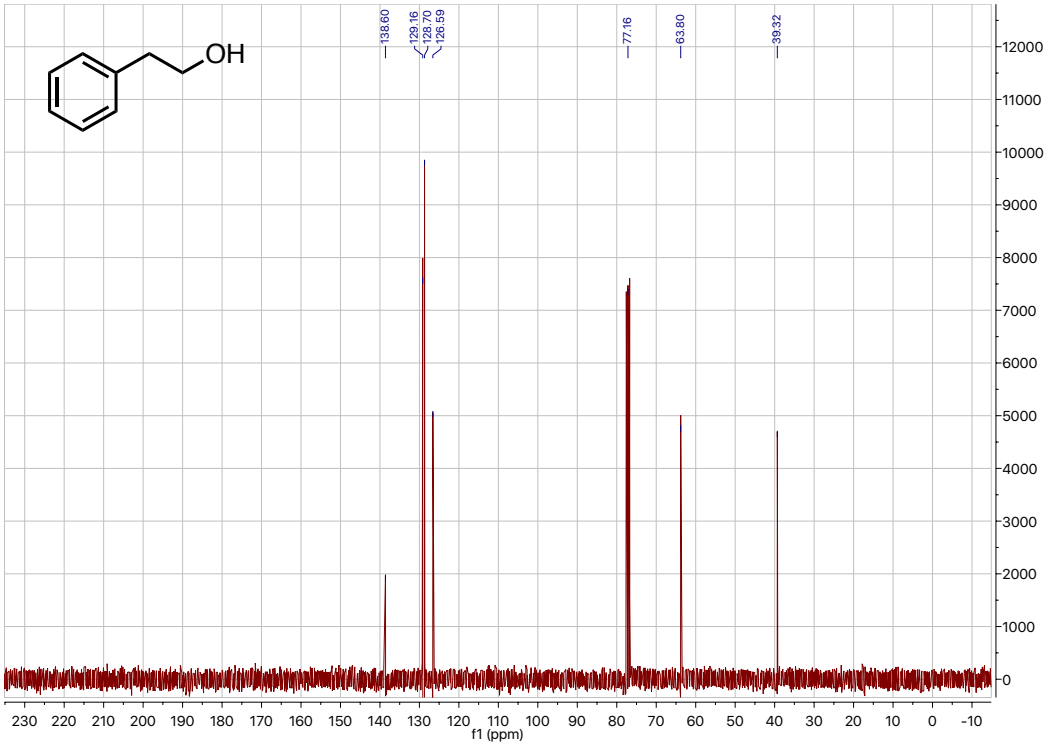

^{1}H NMR: 2-(4-chlorophenyl)ethanol (**8**)

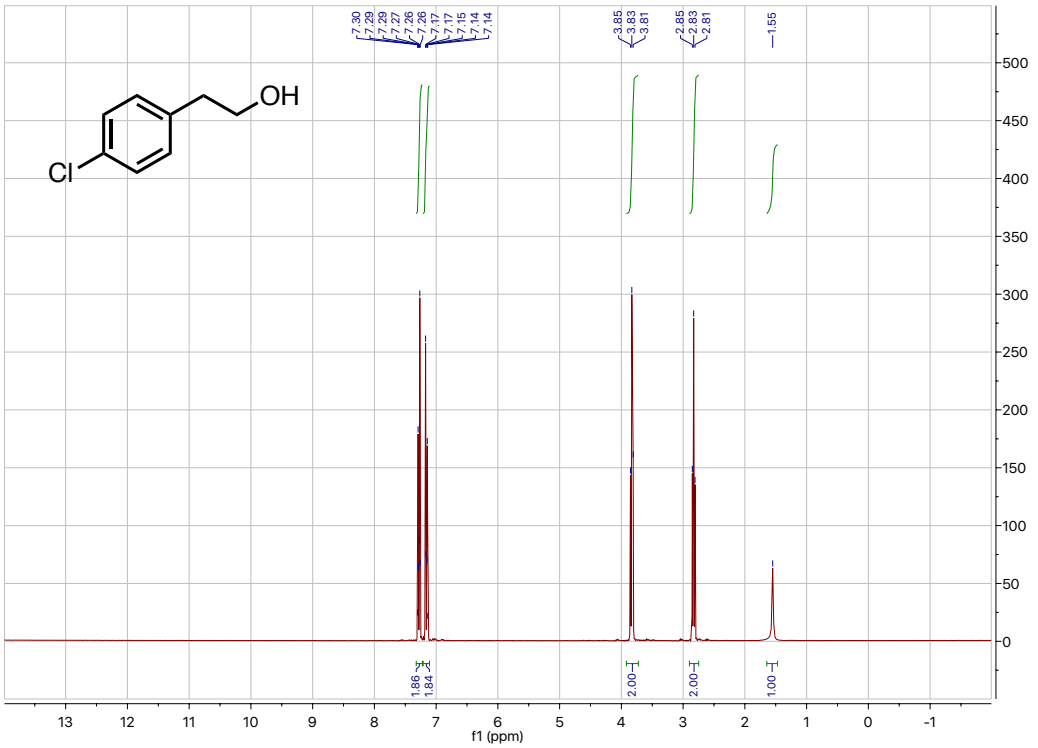

^{13}C NMR: 2-(4-chlorophenyl)ethanol (**8**)

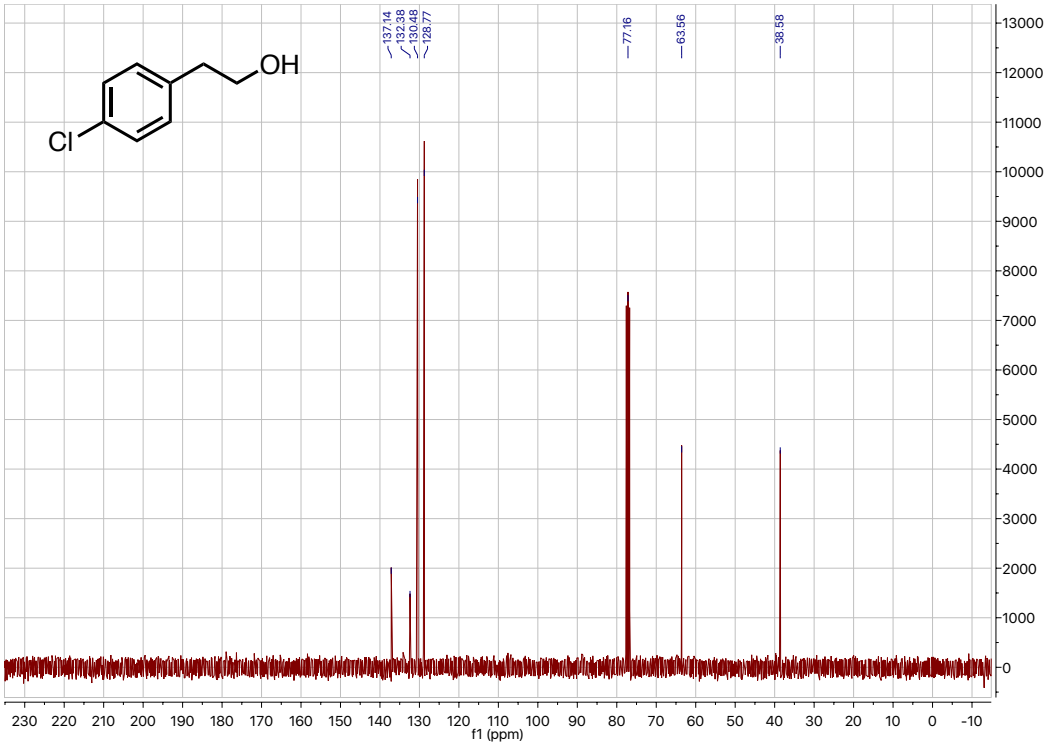

^{1}H NMR: 2-[4-(trifluoromethyl)phenyl]ethanol (**9**)

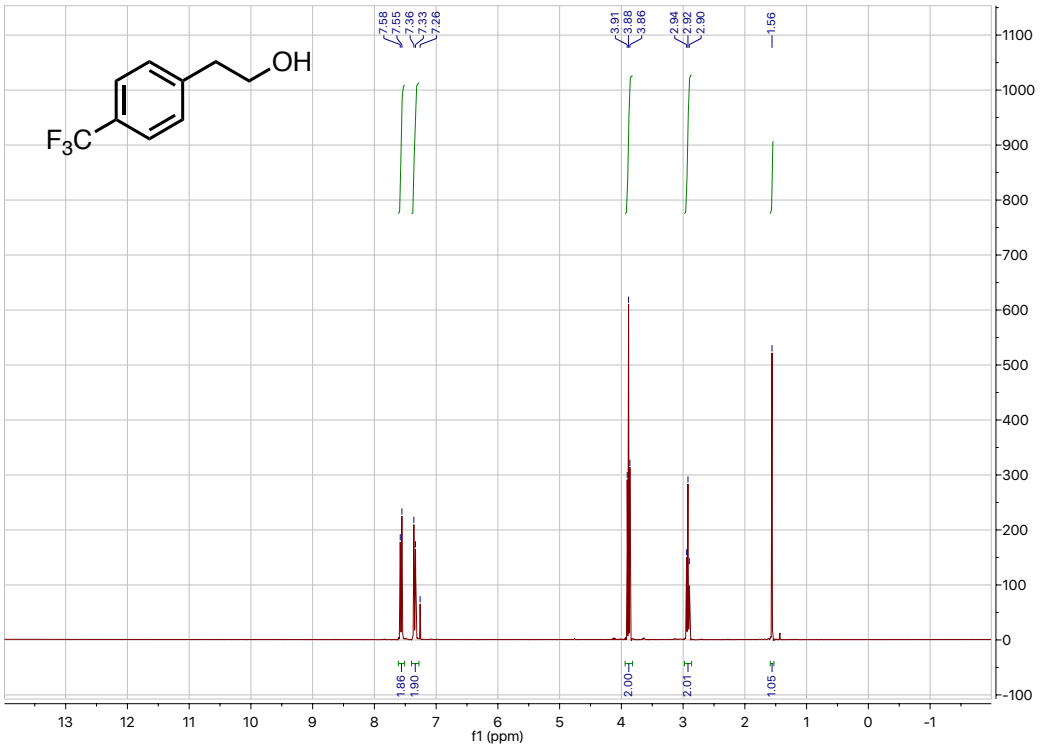

^{13}C NMR: 2-[4-(trifluoromethyl)phenyl]ethanol (**9**)

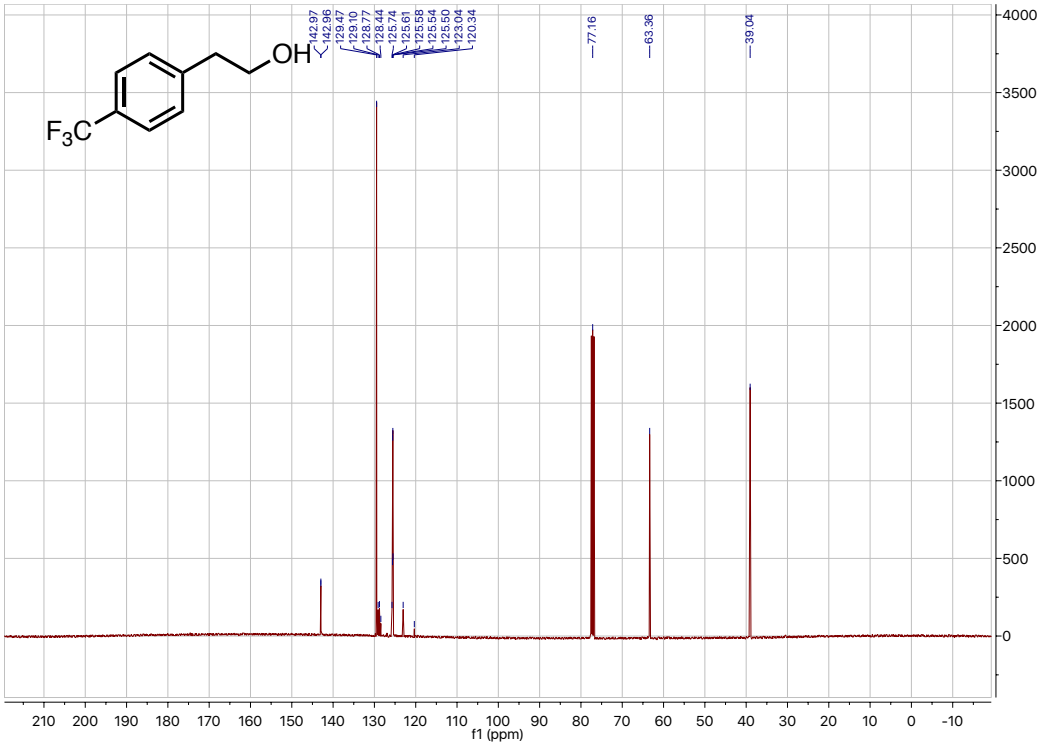

^{19}F NMR: 2-[4-(trifluoromethyl)phenyl]ethanol (**9**)

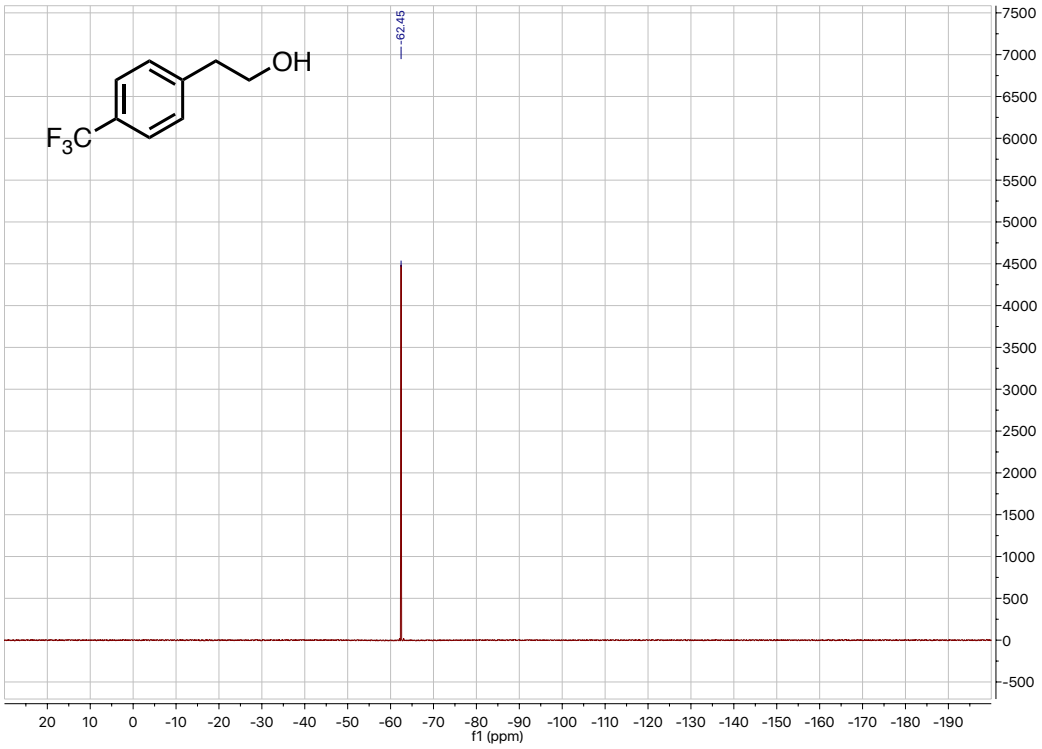

^{1}H NMR: 2-(3-chlorophenyl)ethanol (**10**)

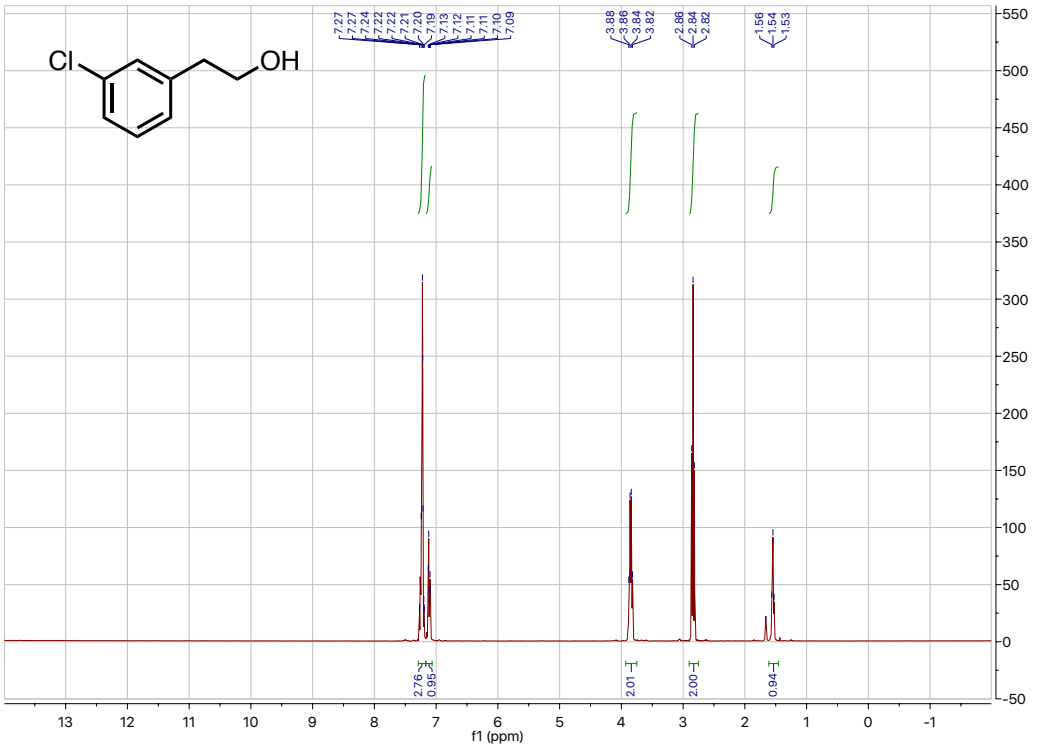

^{13}C NMR: 2-(3-chlorophenyl)ethanol (**10**)

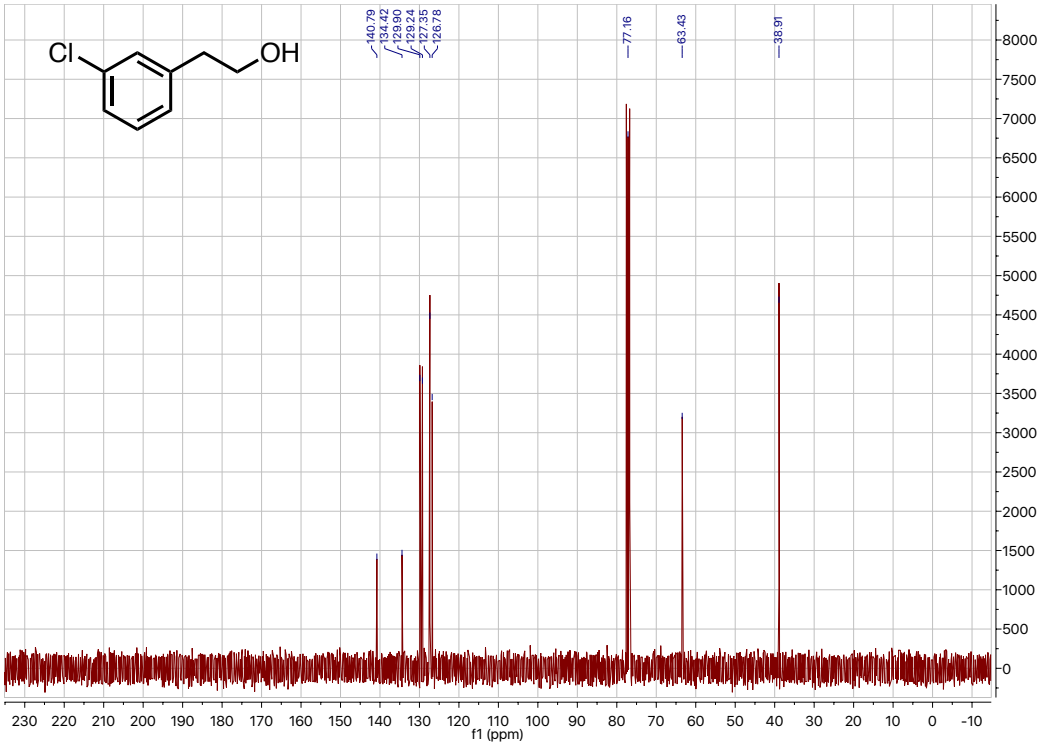

^{1}H NMR: 2-(4-methylphenyl)ethanol (**11**)

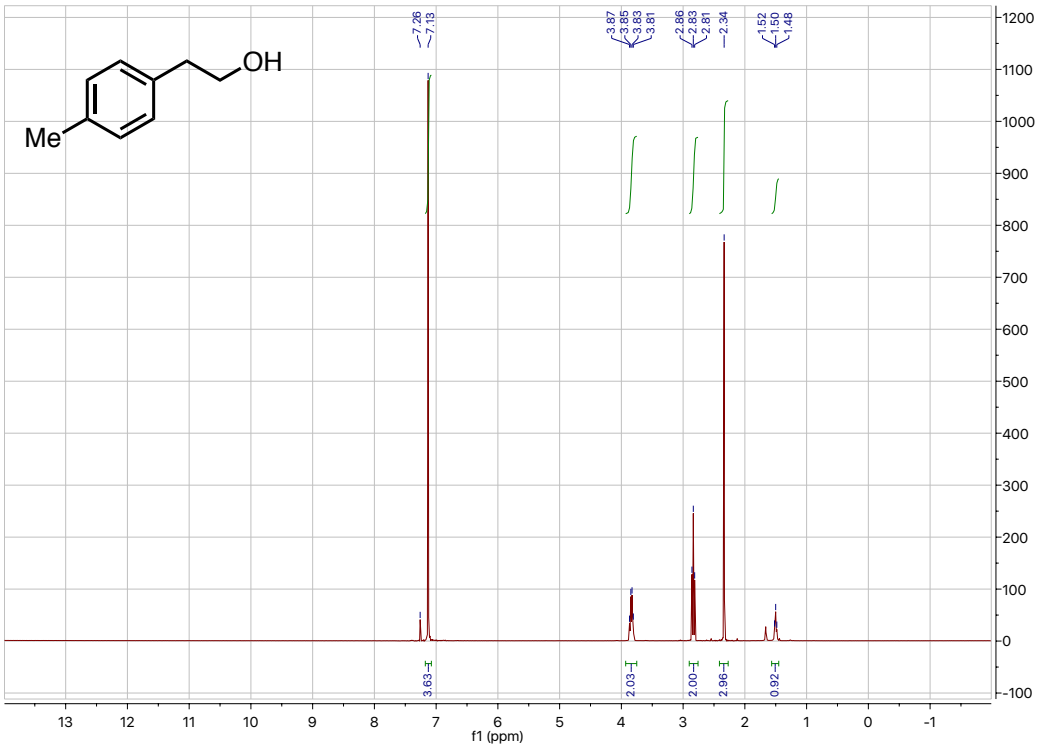

^{13}C NMR: 2-(4-methylphenyl)ethanol (**11**)

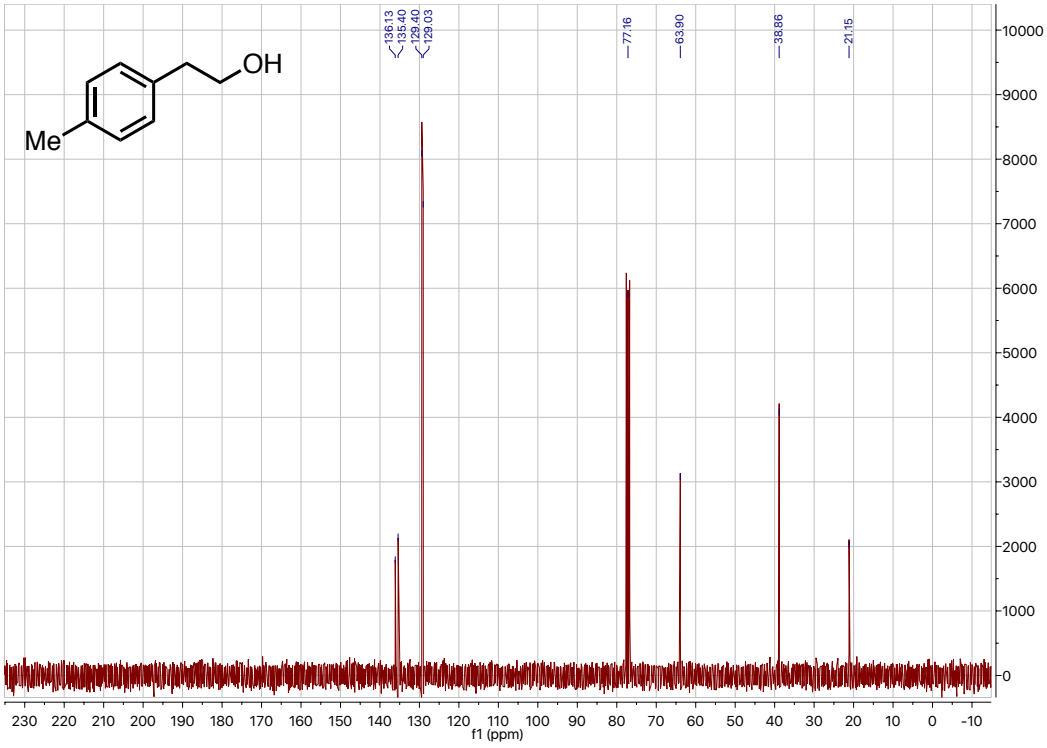

^{1}H NMR: 2-(4-bromophenyl)ethanol (**12**)

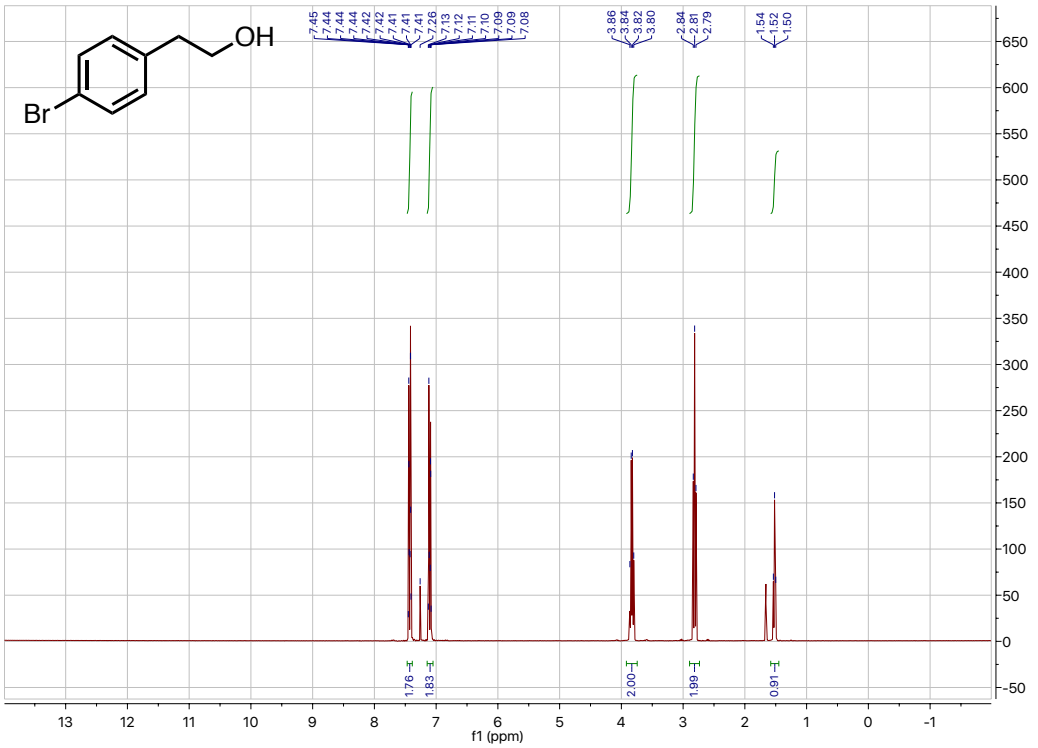

^{13}C NMR: 2-(4-bromophenyl)ethanol (**12**)

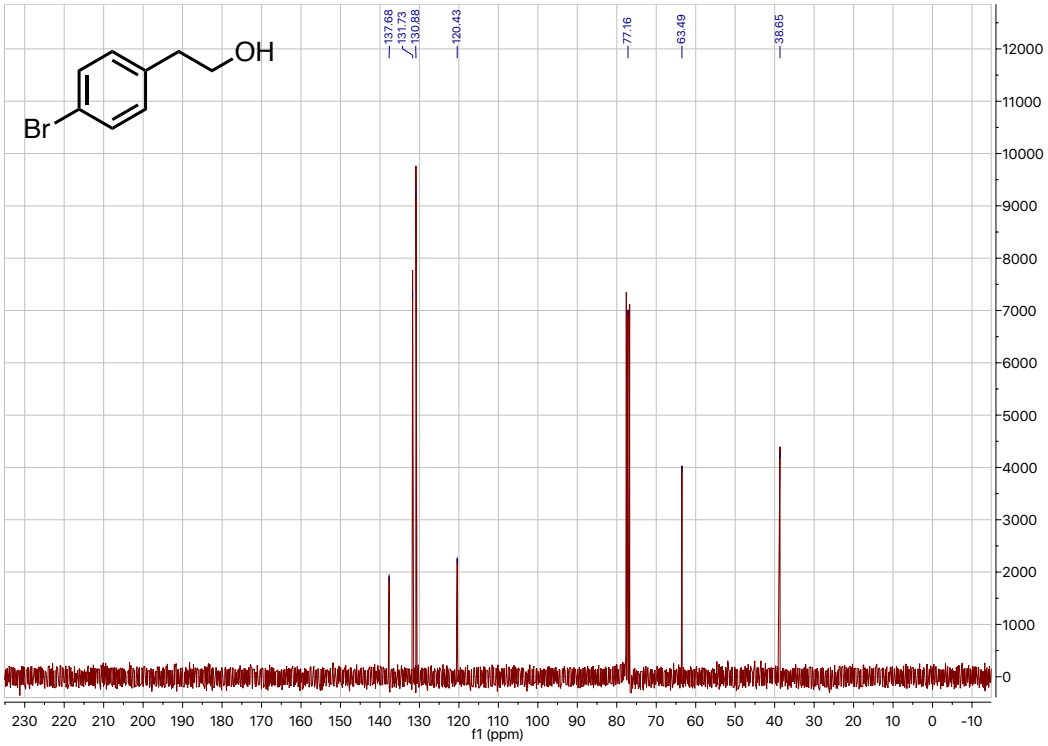

^{1}H NMR: 2-[3-(trifluoromethyl)phenyl]ethanol (**13**)

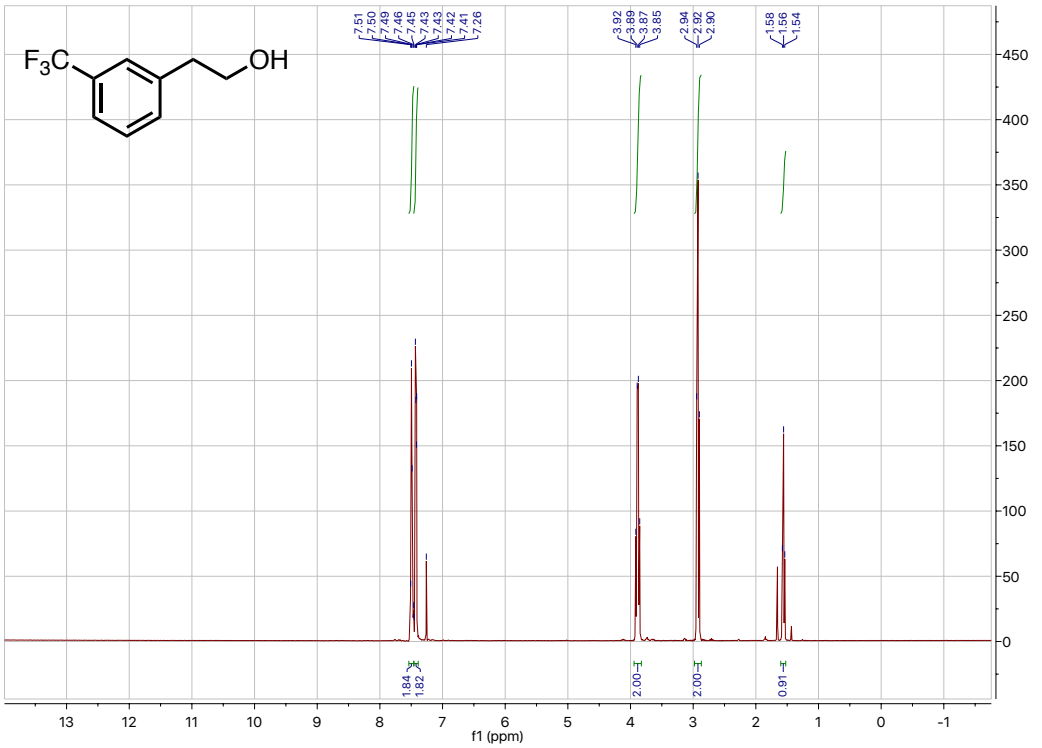

^{13}C NMR: 2-[3-(trifluoromethyl)phenyl]ethanol (**13**)

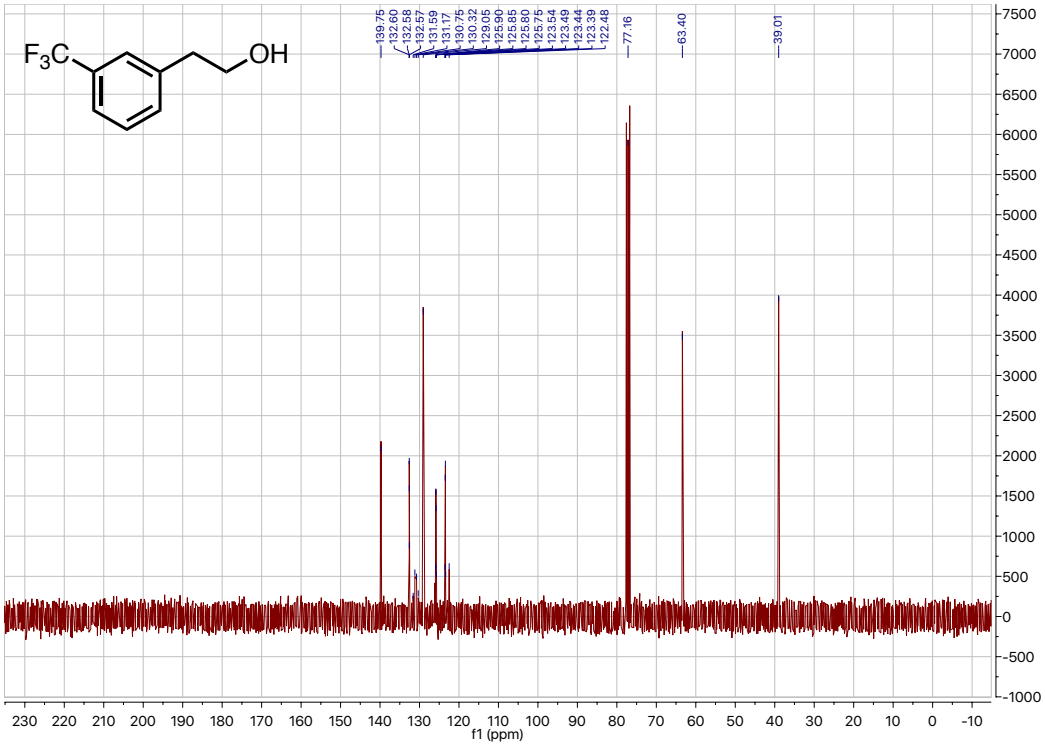

^{19}F NMR: 2-[3-(trifluoromethyl)phenyl]ethanol (**13**)

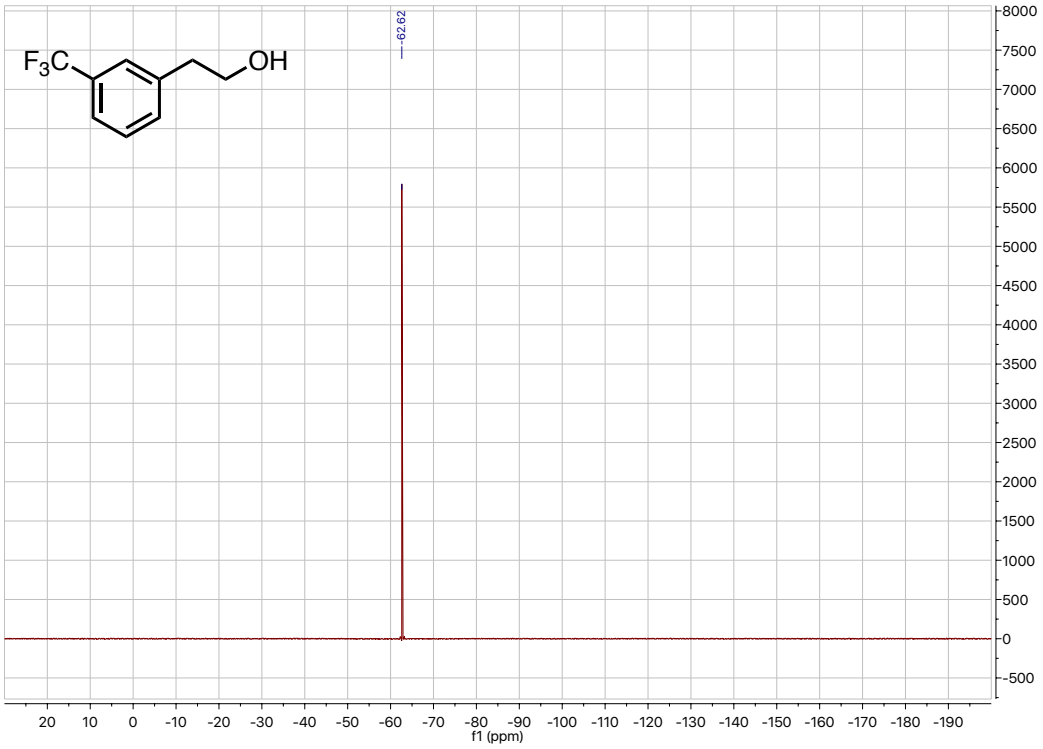

^{1}H NMR: 2-[2-(trifluoromethyl)phenyl]ethanol (**14**)

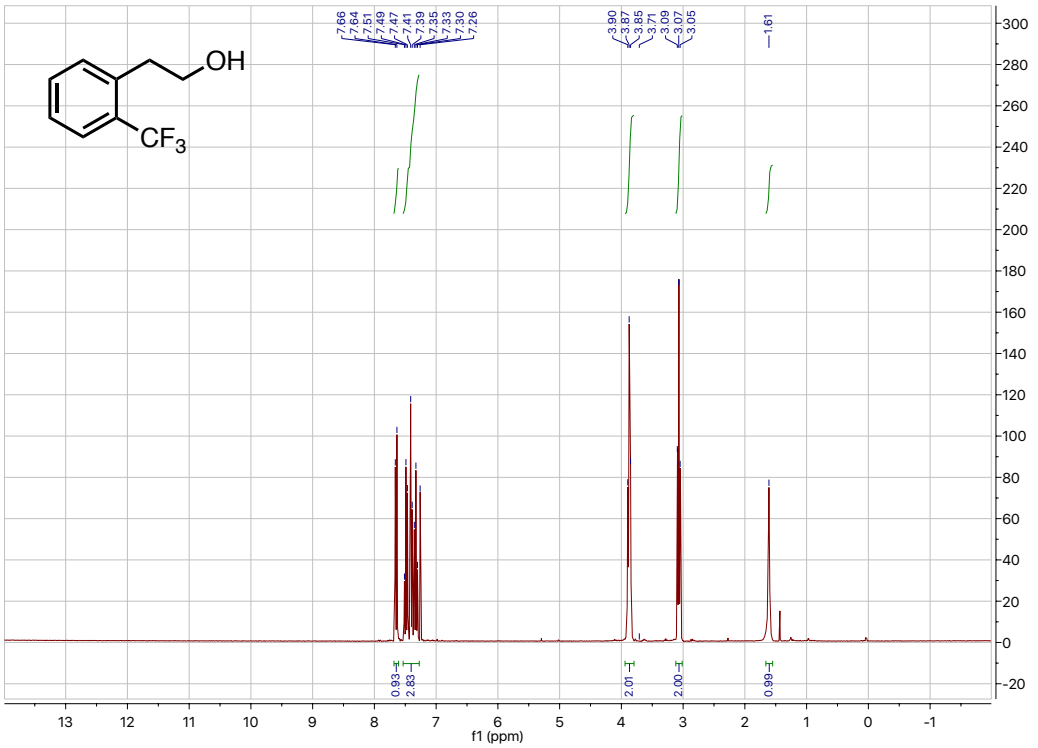

^{13}C NMR: 2-[2-(trifluoromethyl)phenyl]ethanol (**14**)

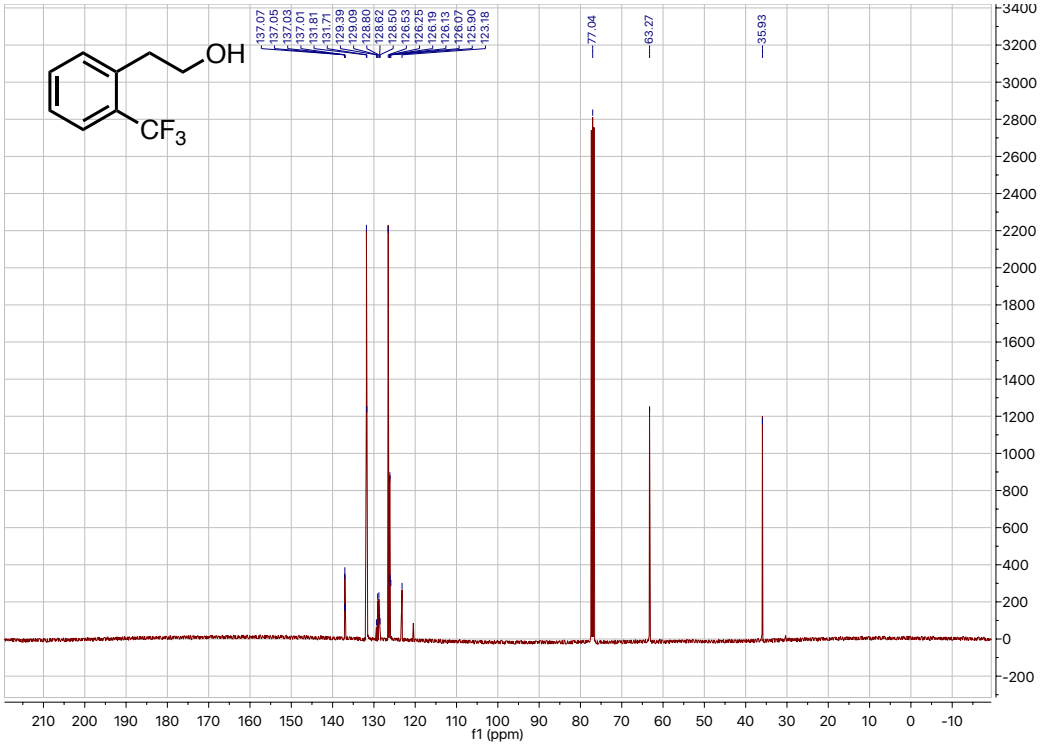

^{19}F NMR: 2-[2-(trifluoromethyl)phenyl]ethanol (**14**)

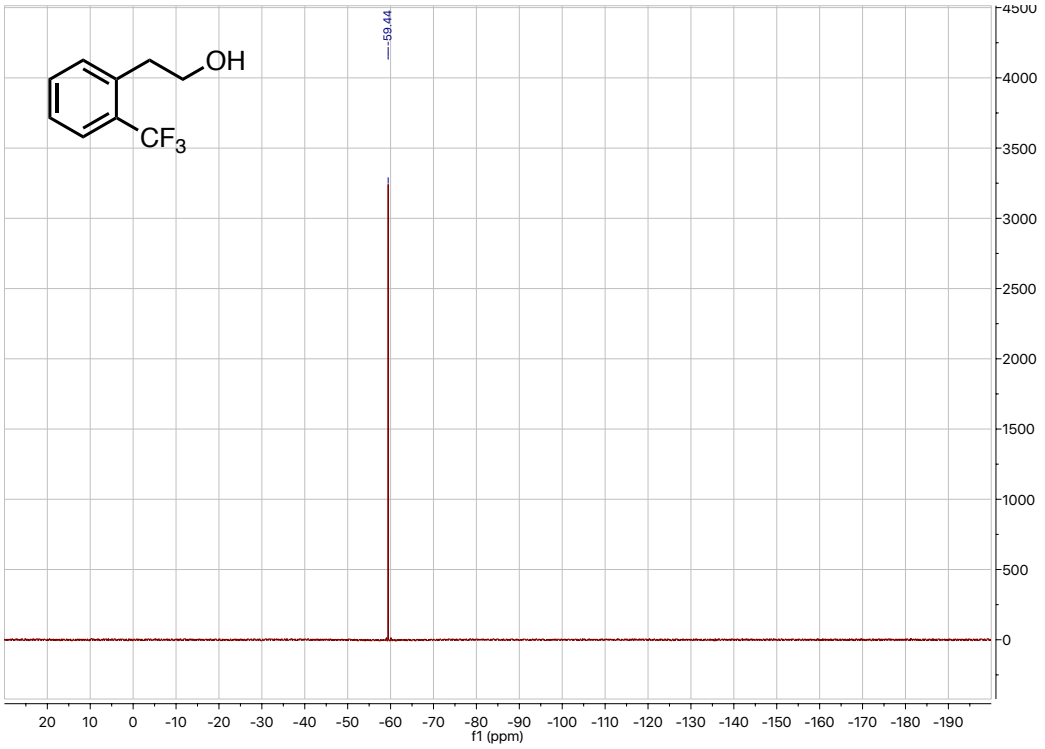

^{1}H NMR: 2-phenyl-1-propanol (**15**)

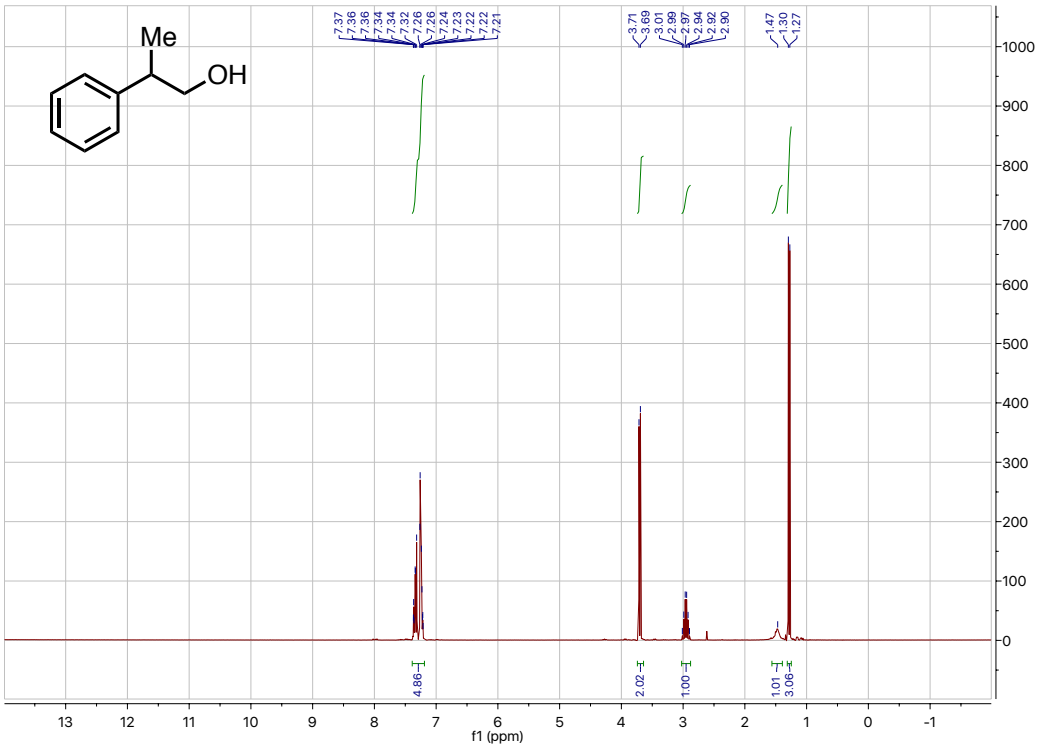

^{13}C NMR: 2-phenyl-1-propanol (**15**)

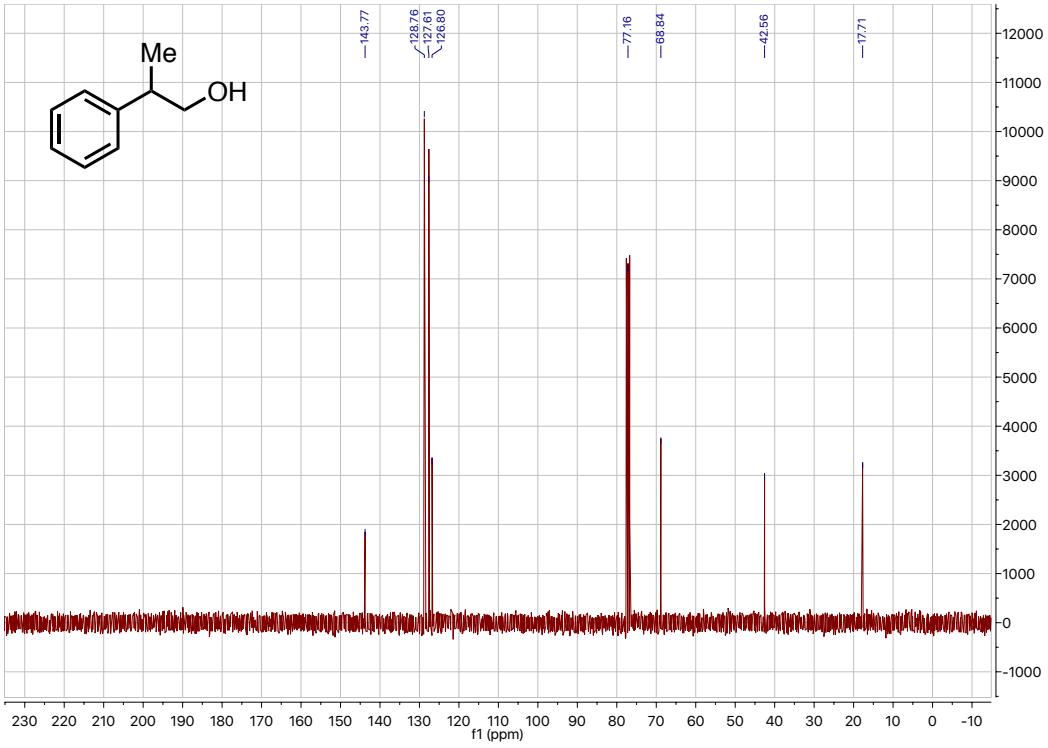

^{1}H NMR: 1-phenyl-2-propanol (**16**)

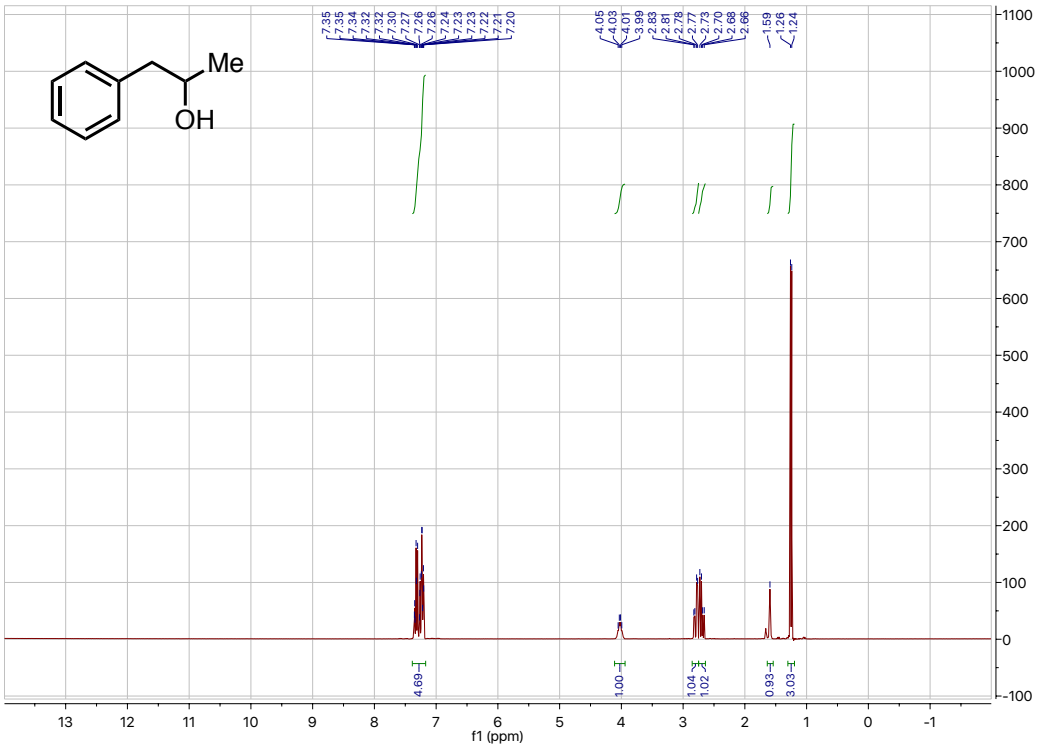

^{13}C NMR: 1-phenyl-2-propanol (**16**)

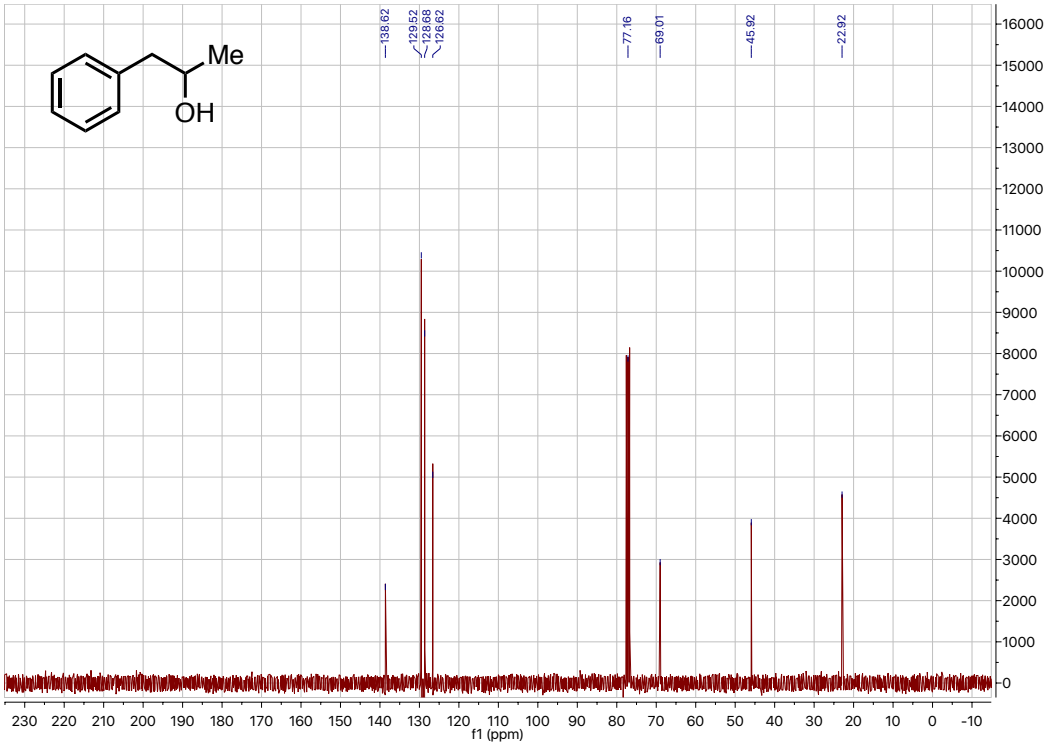

References and Notes

1. T. Punniyamurthy, S. Velusamy, J. Iqbal, Recent advances in transition metal catalyzed oxidation of organic substrates with molecular oxygen. *Chem. Rev.* **105**, 2329–2364 (2005). doi:10.1021/cr050523v Medline

2. J. J. Dong, W. R. Browne, B. L. Feringa, Palladium-catalyzed anti-Markovnikov oxidation of terminal alkenes. *Angew. Chem. Int. Ed.* **54**, 734–744 (2015). doi:10.1002/anie.201404856 Medline

3. M. Beller, J. Seayad, A. Tillack, H. Jiao, Catalytic Markovnikov and anti-Markovnikov functionalization of alkenes and alkynes: Recent developments and trends. *Angew. Chem. Int. Ed.* **43**, 3368–3398 (2004). doi:10.1002/anie.200300616 Medline

4. R. H. Holm, Metal-centered oxygen atom transfer reactions. *Chem. Rev.* **87**, 1401–1449 (1987). doi:10.1021/cr00082a005

5. K. A. Jørgensen, Transition-metal-catalyzed epoxidations. *Chem. Rev.* **89**, 431–458 (1989). doi:10.1021/cr00093a001

6. W. Zhang, J. L. Loebach, S. R. Wilson, E. N. Jacobsen, Enantioselective epoxidation of olefins catalyzed by (salen)manganese complexes. *J. Am. Chem. Soc.* **112**, 2801–2803 (1990). doi:10.1021/ja00163a052

7. J. T. Groves, R. S. Myers, Catalytic asymmetric epoxidations with chiral iron porphyrins. *J. Am. Chem. Soc.* **105**, 5791–5796 (1983). doi:10.1021/ja00356a016

8. D. Ostovic, T. C. Bruice, Mechanism of alkene epoxidation by iron, chromium, and manganese higher valent oxo-metalloporphyrins. *Acc. Chem. Res.* **25**, 314–320 (1992). doi:10.1021/ar00019a007

9. S. P. de Visser, F. Ogliaro, N. Harris, S. Shaik, Multi-state epoxidation of ethene by cytochrome P450: A quantum chemical study. *J. Am. Chem. Soc.* **123**, 3037–3047 (2001). doi:10.1021/ja003544+ Medline

10. R. R. Knowles, E. N. Jacobsen, Attractive noncovalent interactions in asymmetric catalysis: Links between enzymes and small molecule catalysts. *Proc. Natl. Acad. Sci. U.S.A.* **107**, 20678–20685 (2010). doi:10.1073/pnas.1006402107 Medline

11. D. J. Miller, R. K. Allemann, Sesquiterpene synthases: Passive catalysts or active players? *Nat. Prod. Rep.* **29**, 60–71 (2012). doi:10.1039/C1NP00060H Medline

12. K. U. Wendt, G. E. Schulz, E. J. Corey, D. R. Liu, Enzyme mechanisms for polycyclic triterpene formation. *Angew. Chem. Int. Ed.* **39**, 2812–2833 (2000). Medline

13. W. Buckel, B. T. Golding, Radical enzymes in anaerobes. *Annu. Rev. Microbiol.* **60**, 27–49 (2006). doi:10.1146/annurev.micro.60.080805.142216 Medline

14. R. G. Rosenthal, B. Vögeli, T. Wagner, S. Shima, T. J. Erb, A conserved threonine prevents self-intoxication of enoyl-thioester reductases. *Nat. Chem. Biol.* **13**, 745–749 (2017). doi:10.1038/nchembio.2375 Medline

15. P. R. Ortiz De Montellano, *Cytochrome P450: Structure, Mechanism, and Biochemistry* (Springer, 2005).

16. F. P. Guengerich, A. W. Munro, Unusual cytochrome P450 enzymes and reactions. *J. Biol. Chem.* **288**, 17065–17073 (2013). doi:10.1074/jbc.R113.462275 Medline

17. S. P. de Visser, D. Kumar, S. Shaik, How do aldehyde side products occur during alkene epoxidation by cytochrome P450? Theory reveals a state-specific multi-state scenario where the high-spin component leads to all side products. *J. Inorg. Biochem.* **98**, 1183–1193 (2004). doi:10.1016/j.jinorgbio.2004.01.015 Medline

18. Y.-C. Yin, H.-L. Yu, Z.-J. Luan, R.-J. Li, P.-F. Ouyang, J. Liu, J.-H. Xu, Unusually broad substrate profile of self-sufficient cytochrome P450 monooxygenase CYP116B4 from *Labrenzia aggregata*. *ChemBioChem* **15**, 2443–2449 (2014). doi:10.1002/cbic.201402309 Medline

19. F. H. Arnold, Design by directed evolution. *Acc. Chem. Res.* **31**, 125–131 (1998). doi:10.1021/ar960017f

20. K. Chockalingam, Z. Chen, J. A. Katzenellenbogen, H. Zhao, Directed evolution of specific receptor-ligand pairs for use in the creation of gene switches. *Proc. Natl. Acad. Sci. U.S.A.* **102**, 5691–5696 (2005). doi:10.1073/pnas.0409206102 Medline

21. M. T. Reetz, J. D. Carballeira, Iterative saturation mutagenesis (ISM) for rapid directed evolution of functional enzymes. *Nat. Protoc.* **2**, 891–903 (2007). doi:10.1038/nprot.2007.72 Medline

22. S. P. Thomas, V. K. Aggarwal, Asymmetric hydroboration of 1,1-disubstituted alkenes. *Angew. Chem. Int. Ed.* **48**, 1896–1898 (2009). doi:10.1002/anie.200805604 Medline

23. It is likely that highly (*R*)- and (*S*)-selective variants for anti-Markovnikov oxidation could be obtained by further evolution of the enzyme, as has been demonstrated with other P450-based catalysts (*24*).

24. M. T. Reetz, Laboratory evolution of stereoselective enzymes: A prolific source of catalysts for asymmetric reactions. *Angew. Chem. Int. Ed.* **50**, 138–174 (2011). doi:10.1002/anie.201000826 Medline

25. B. M. Trost, T. Yasukata, A catalytic asymmetric Wagner-Meerwein shift. *J. Am. Chem. Soc.* **123**, 7162–7163 (2001). doi:10.1021/ja010504c Medline

26. H. Wu, Q. Wang, J. Zhu, Organocatalytic enantioselective vinylogous pinacol rearrangement enabled by chiral ion pairing. *Angew. Chem. Int. Ed.* **55**, 15411–15414 (2016). doi:10.1002/anie.201609911 Medline

27. T. J. Erb, P. R. Jones, A. Bar-Even, Synthetic metabolism: Metabolic engineering meets enzyme design. *Curr. Opin. Chem. Biol.* **37**, 56–62 (2017). doi:10.1016/j.cbpa.2016.12.023 Medline

28. J. Haggin, Chemists seek greater recognition for catalysis. *Chem. Eng. News* **71**, 23–27 (1993). doi:10.1021/cen-v071n022.p023

29. G. Dong, P. Teo, Z. K. Wickens, R. H. Grubbs, Primary alcohols from terminal olefins: Formal anti-Markovnikov hydration via triple relay catalysis. *Science* **333**, 1609–1612 (2011). doi:10.1126/science.1208685 Medline

30. X. Hu, G. Zhang, F. Bu, A. Lei, Visible-light mediated anti-Markovnikov hydration of olefins. *ACS Catal.* **7**, 1432–1437 (2017). doi:10.1021/acscatal.6b03388

31. S. Wu, J. Liu, Z. Li, Biocatalytic formal anti-Markovnikov hydroamination and hydration of aryl alkenes. *ACS Catal.* **7**, 5225–5233 (2017). doi:10.1021/acscatal.7b01464

32. E. R. Burkhardt, K. Matos, Boron reagents in process chemistry: Excellent tools for selective reductions. *Chem. Rev.* **106**, 2617–2650 (2006). doi:10.1021/cr0406918 Medline

33. J. Murciano-Calles, D. K. Romney, S. Brinkmann-Chen, A. R. Buller, F. H. Arnold, A panel of TrpB biocatalysts derived from tryptophan synthase through the transfer of mutations that mimic allosteric activation. *Angew. Chem. Int. Ed.* **55**, 11577–11581 (2016). doi:10.1002/anie.201606242 Medline

34. D. K. Romney, J. Murciano-Calles, J. E. Wehrmüller, F. H. Arnold, Unlocking reactivity of TrpB: A general biocatalytic platform for synthesis of tryptophan analogues. *J. Am. Chem. Soc.* **139**, 10769–10776 (2017). doi:10.1021/jacs.7b05007 Medline

35. B. M. Nestl, S. C. Hammer, B. A. Nebel, B. Hauer, New generation of biocatalysts for organic synthesis. *Angew. Chem. Int. Ed.* **53**, 3070–3095 (2014). doi:10.1002/anie.201302195 Medline

36. G.-D. Roiban, M. T. Reetz, Expanding the toolbox of organic chemists: Directed evolution of P450 monooxygenases as catalysts in regio- and stereoselective oxidative hydroxylation. *Chem. Commun. (Camb.)* **51**, 2208–2224 (2015). doi:10.1039/C4CC09218J Medline

37. D. Mansuy, J. Leclaire, M. Fontecave, M. Momenteau, Oxidation of monosubstituted olefins by cytochromes P-450 and heme models: Evidence for the formation of aldehydes in addition to epoxides and allylic alcohols. *Biochem. Biophys. Res. Commun.* **119**, 319–325 (1984). doi:10.1016/0006-291X(84)91654-1 Medline

38. V. P. Miller, J. A. Fruetel, P. R. Ortiz de Montellano, Cytochrome P450cam-catalyzed oxidation of a hypersensitive radical probe. *Arch. Biochem. Biophys.* **298**, 697–702 (1992). doi:10.1016/0003-9861(92)90468-C Medline

39. W. Engel, Detection of a "nonaromatic" NIH shift during in vivo metabolism of the monoterpene carvone in humans. *J. Agric. Food Chem.* **50**, 1686–1694 (2002). doi:10.1021/jf011199h Medline

40. Styrene derivatives are special alkenes because of their conjugation with an aromatic system that might support metal-oxo–mediated anti-Markovnikov oxidation by stabilizing a carbocation at the benzylic position. Further engineering of the *L. aggregata* P450 or other monooxygenases will reveal whether the aMOx cycle can operate efficiently on aliphatic alkenes.

41. S. C. Hammer, A. M. Knight, F. H. Arnold, Design and evolution of enzymes for non-natural chemistry. *Curr. Opin. Green Sustain. Chem.* **7**, 23–30 (2017). doi:10.1016/j.cogsc.2017.06.002

42. C. K. Prier, F. H. Arnold, Chemomimetic biocatalysis: Exploiting the synthetic potential of cofactor-dependent enzymes to create new catalysts. *J. Am. Chem. Soc.* **137**, 13992–14006 (2015). doi:10.1021/jacs.5b09348 Medline

43. M. D. Truppo, Biocatalysis in the pharmaceutical industry: The need for speed. *ACS Med. Chem. Lett.* **8**, 476–480 (2017). doi:10.1021/acsmedchemlett.7b00114 Medline

44. A. X. Gao, S. B. Thomas, S. A. Snyder, in *Molecular Rearrangements in Organic Synthesis*, C. M. Rojas, Ed. (Wiley, 2015), pp. 2–33.

45. D. G. Gibson, L. Young, R.-Y. Chuang, J. C. Venter, C. A. Hutchison 3rd, H. O. Smith, Enzymatic assembly of DNA molecules up to several hundred kilobases. *Nat. Methods* **6**, 343–345 (2009). doi:10.1038/nmeth.1318 Medline

46. S. Kille, C. G. Acevedo-Rocha, L. P. Parra, Z.-G. Zhang, D. J. Opperman, M. T. Reetz, J. P. Acevedo, Reducing codon redundancy and screening effort of combinatorial protein libraries created by saturation mutagenesis. *ACS Synth. Biol.* **2**, 83–92 (2013). doi:10.1021/sb300037w Medline

47. H. B. Hopps, Purpald: A reagent that turns aldehydes purple. *Aldrichim Acta* **33**, 28–30 (2000).

48. F. P. Guengerich, M. V. Martin, C. D. Sohl, Q. Cheng, Measurement of cytochrome P450 and NADPH-cytochrome P450 reductase. *Nat. Protoc.* **4**, 1245–1251 (2009). doi:10.1038/nprot.2009.121 Medline

49. P. Teo, Z. K. Wickens, G. Dong, R. H. Grubbs, Efficient and highly aldehyde selective Wacker oxidation. *Org. Lett.* **14**, 3237–3239 (2012). doi:10.1021/ol301240g Medline

50. Z. K. Wickens, B. Morandi, R. H. Grubbs, Aldehyde-selective Wacker-type oxidation of unbiased alkenes enabled by a nitrite co-catalyst. *Angew. Chem. Int. Ed.* **52**, 11257–11260 (2013). doi:10.1002/anie.201306756 Medline

51. Z. K. Wickens, K. Skakuj, B. Morandi, R. H. Grubbs, Catalyst-controlled Wacker-type oxidation: Facile access to functionalized aldehydes. *J. Am. Chem. Soc.* **136**, 890–893 (2014). doi:10.1021/ja411749k Medline

52. C. K. Chu, D. T. Ziegler, B. Carr, Z. K. Wickens, R. H. Grubbs, Direct access to β-fluorinated aldehydes by nitrite-modified Wacker oxidation. *Angew. Chem. Int. Ed.* **55**, 8435–8439 (2016). doi:10.1002/anie.201603424 Medline

53. K. E. Kim, J. Li, R. H. Grubbs, B. M. Stoltz, Catalytic anti-Markovnikov transformations of hindered terminal alkenes enabled by aldehyde-selective Wacker-type oxidation. *J. Am. Chem. Soc.* **138**, 13179–13182 (2016). doi:10.1021/jacs.6b08788 Medline

54. S. Nakaoka, Y. Murakami, Y. Kataoka, Y. Ura, Maleimide-assisted anti-Markovnikov Wacker-type oxidation of vinylarenes using molecular oxygen as a terminal oxidant. *Chem. Commun. (Camb.)* **52**, 335–338 (2016). doi:10.1039/C5CC06746D Medline

55. J. Chen, C.-M. Che, A practical and mild method for the highly selective conversion of terminal alkenes into aldehydes through epoxidation-isomerization with ruthenium(IV)-porphyrin catalysts. *Angew. Chem. Int. Ed.* **43**, 4950–4954 (2004). doi:10.1002/anie.200460545 Medline

56. G. Jiang, J. Chen, H.-Y. Thu, J.-S. Huang, N. Zhu, C.-M. Che, Ruthenium porphyrin-catalyzed aerobic oxidation of terminal aryl alkenes to aldehydes by a tandem epoxidation-isomerization pathway. *Angew. Chem. Int. Ed.* **47**, 6638–6642 (2008). doi:10.1002/anie.200801500 Medline

57. J. A. Wright, M. J. Gaunt, J. B. Spencer, Novel anti-Markovnikov regioselectivity in the Wacker reaction of styrenes. *Chemistry* **12**, 949–955 (2006). doi:10.1002/chem.200400644 Medline

58. B. Weiner, A. Baeza, T. Jerphagnon, B. L. Feringa, Aldehyde selective Wacker oxidations of phthalimide protected allylic amines: A new catalytic route to β3-amino acids. *J. Am. Chem. Soc.* **131**, 9473–9474 (2009). doi:10.1021/ja902591g Medline

59. J. J. Dong, M. Fañanás-Mastral, P. L. Alsters, W. R. Browne, B. L. Feringa, Palladium-catalyzed selective anti-Markovnikov oxidation of allylic esters. *Angew. Chem. Int. Ed.* **52**, 5561–5565 (2013). doi:10.1002/anie.201301809 Medline

60. J. J. Dong, E. C. Harvey, M. Fañanás-Mastral, W. R. Browne, B. L. Feringa, Palladium-catalyzed anti-Markovnikov oxidation of allylic amides to protected β-amino aldehydes. *J. Am. Chem. Soc.* **136**, 17302–17307 (2014). doi:10.1021/ja510163w Medline

61. G.-Q. Chen, Z.-J. Xu, C.-Y. Zhou, C.-M. Che, Selective oxidation of terminal aryl and aliphatic alkenes to aldehydes catalyzed by iron(III) porphyrins with triflate as a counter anion. *Chem. Commun. (Camb.)* **47**, 10963–10965 (2011). doi:10.1039/c1cc13574k Medline

62. A. D. Chowdhury, R. Ray, G. K. Lahiri, An iron catalyzed regioselective oxidation of terminal alkenes to aldehydes. *Chem. Commun. (Camb.)* **48**, 5497–5499 (2012). doi:10.1039/c2cc32051g Medline

63. G. Zhang, X. Hu, C.-W. Chiang, H. Yi, P. Pei, A. K. Singh, A. Lei, Anti-Markovnikov oxidation of β-alkyl styrenes with H_2O as the terminal oxidant. *J. Am. Chem. Soc.* **138**, 12037–12040 (2016). doi:10.1021/jacs.6b07411 Medline

64. J. Yang, R. Yan, A. Roy, D. Xu, J. Poisson, Y. Zhang, The I-TASSER Suite: Protein structure and function prediction. *Nat. Methods* **12**, 7–8 (2015). doi:10.1038/nmeth.3213 Medline

65. L. Bordoli, F. Kiefer, K. Arnold, P. Benkert, J. Battey, T. Schwede, Protein structure homology modeling using SWISS-MODEL workspace. *Nat. Protoc.* **4**, 1–13 (2009). doi:10.1038/nprot.2008.197 Medline

66. L. A. Kelley, S. Mezulis, C. M. Yates, M. N. Wass, M. J. E. Sternberg, The Phyre2 web portal for protein modeling, prediction and analysis. *Nat. Protoc.* **10**, 845–858 (2015). doi:10.1038/nprot.2015.053 Medline

67. S. Li, M. R. Chaulagain, A. R. Knauff, L. M. Podust, J. Montgomery, D. H. Sherman, Selective oxidation of carbolide C–H bonds by an engineered macrolide P450 mono-oxygenase. *Proc. Natl. Acad. Sci. U.S.A.* **106**, 18463–18468 (2009). doi:10.1073/pnas.0907203106 Medline

68. C. W. Lee, J.-H. Lee, H. Rimal, H. Park, J. H. Lee, T.-J. Oh, Crystal structure of cytochrome P450 (CYP105P2) from *Streptomyces peucetius* and its conformational changes in response to substrate binding. *Int. J. Mol. Sci.* **17**, 813–822 (2016). doi:10.3390/ijms17060813 Medline

69. S. P. France, L. J. Hepworth, N. J. Turner, S. L. Flitsch, Constructing biocatalytic cascades: In vitro and in vivo approaches to de novo multi-enzyme pathways. *ACS Catal.* **7**, 710–724 (2016). doi:10.1021/acscatal.6b02979

70. M. Hall, A. S. Bommarius, Enantioenriched compounds via enzyme-catalyzed redox reactions. *Chem. Rev.* **111**, 4088–4110 (2011). doi:10.1021/cr200013n Medline

71. P. Könst, H. Merkens, S. Kara, S. Kochius, A. Vogel, R. Zuhse, D. Holtmann, I. W. C. E. Arends, F. Hollmann, Enantioselective oxidation of aldehydes catalyzed by alcohol dehydrogenase. *Angew. Chem. Int. Ed.* **51**, 9914–9917 (2012). doi:10.1002/anie.201203219 Medline

72. S. M. McKenna, S. Leimkühler, S. Herter, N. J. Turner, A. J. Carnell, Enzyme cascade reactions: Synthesis of furandicarboxylic acid (FDCA) and carboxylic acids using oxidases in tandem. *Green Chem.* **17**, 3271–3275 (2015). doi:10.1039/C5GC00707K

73. J. Mangas-Sanchez, S. P. France, S. L. Montgomery, G. A. Aleku, H. Man, M. Sharma, J. I. Ramsden, G. Grogan, N. J. Turner, Imine reductases (IREDs). *Curr. Opin. Chem. Biol.* **37**, 19–25 (2017). doi:10.1016/j.cbpa.2016.11.022 Medline

74. G. A. Aleku, S. P. France, H. Man, J. Mangas-Sanchez, S. L. Montgomery, M. Sharma, F. Leipold, S. Hussain, G. Grogan, N. J. Turner, A reductive aminase from *Aspergillus oryza*e. *Nat. Chem.* **9**, 961–969 (2017). doi:10.1038/nchem.2782

75. H. Lechner, D. Pressnitz, W. Kroutil, Biocatalysts for the formation of three- to six-membered carbo- and heterocycles. *Biotechnol. Adv.* **33**, 457–480 (2015). doi:10.1016/j.biotechadv.2015.01.012 Medline

76. M. Brovetto, D. Gamenara, P. Saenz Méndez, G. A. Seoane, C–C bond-forming lyases in organic synthesis. *Chem. Rev.* **111**, 4346–4403 (2011). doi:10.1021/cr100299p Medline

77. M. Müller, G. A. Sprenger, M. Pohl, C–C bond formation using ThDP-dependent lyases. *Curr. Opin. Chem. Biol.* **17**, 261–270 (2013). doi:10.1016/j.cbpa.2013.02.017 Medline

78. C. L. Windle, M. Müller, A. Nelson, A. Berry, Engineering aldolases as biocatalysts. *Curr. Opin. Chem. Biol.* **19**, 25–33 (2014). doi:10.1016/j.cbpa.2013.12.010 Medline

79. O. O. Kovalenko, H. Adolfsson, Highly efficient and chemoselective zinc-catalyzed hydrosilylation of esters under mild conditions. *Chemistry* **21**, 2785–2788 (2015). doi:10.1002/chem.201406176 Medline

80. S. Elangovan, M. Garbe, H. Jiao, A. Spannenberg, K. Junge, M. Beller, Hydrogenation of esters to alcohols catalyzed by defined manganese pincer complexes. *Angew. Chem. Int. Ed.* **55**, 15364–15368 (2016). doi:10.1002/anie.201607233 Medline

81. M. A. Avery, M. Alvim-Gaston, J. A. Vroman, B. Wu, A. Ager, W. Peters, B. L. Robinson, W. Charman, Structure-activity relationships of the antimalarial agent artemisinin. 7. Direct modification of (+)-artemisinin and in vivo antimalarial screening of new, potential preclinical antimalarial candidates. *J. Med. Chem.* **45**, 4321–4335 (2002). doi:10.1021/jm020142z Medline

82. D. Peng, M. Zhang, Z. Huang, A general, practical triethylborane-catalyzed reduction of carbonyl functions to alcohols. *Chemistry* **21**, 14737–14741 (2015). doi:10.1002/chem.201502942 Medline

83. X. Cui, Y. Li, C. Topf, K. Junge, M. Beller, Direct ruthenium-catalyzed hydrogenation of carboxylic acids to alcohols. *Angew. Chem. Int. Ed.* **54**, 10596–10599 (2015). doi:10.1002/anie.201503562 Medline

84. X. Du, Y. Zhang, D. Peng, Z. Huang, Base-metal-catalyzed regiodivergent alkene hydrosilylations. *Angew. Chem. Int. Ed.* **55**, 6671–6675 (2016). doi:10.1002/anie.201601197 Medline